



HAL
open science

Floristic survey, trace element transfers between soil and vegetation and human health risk at an urban industrial wasteland

Jordan Collot, Philippe Binet, Abdoulaye Mahamat Malabad, Benjamin Pauget, Marie-Laure Toussaint, Michel Chalot

► To cite this version:

Jordan Collot, Philippe Binet, Abdoulaye Mahamat Malabad, Benjamin Pauget, Marie-Laure Toussaint, et al.. Floristic survey, trace element transfers between soil and vegetation and human health risk at an urban industrial wasteland. *Journal of Hazardous Materials*, 2023, 459, 10.1016/j.jhazmat.2023.132169 . hal-04707507

HAL Id: hal-04707507

<https://hal.science/hal-04707507v1>

Submitted on 30 Sep 2024

HAL is a multi-disciplinary open access archive for the deposit and dissemination of scientific research documents, whether they are published or not. The documents may come from teaching and research institutions in France or abroad, or from public or private research centers.

L'archive ouverte pluridisciplinaire **HAL**, est destinée au dépôt et à la diffusion de documents scientifiques de niveau recherche, publiés ou non, émanant des établissements d'enseignement et de recherche français ou étrangers, des laboratoires publics ou privés.

1 Floristic survey, trace element transfers between soil and vegetation and human health risk at an urban
2 industrial wasteland.

3 Jordan Collot¹, Philippe Binet¹, Abdoulaye Mahamat Malabad¹, Benjamin Pauget², Marie-Laure
4 Toussaint¹, Michel Chalot^{1,3*}.

5 ¹Chrono-Environnement UMR6249, Université Franche-Comté CNRS, F-25000, Besançon, France.

6 ²TESORA, Le Visium, 22 avenue Aristide Briand, 94110 Arcueil, France.

7 ³Université de Lorraine, Faculté des Sciences et Technologies, Nancy, 54000, France.

8

9 * Corresponding author : michel.chalot@univ-fcomte.fr (M. Chalot).

10

11 Highlights

- 12 • The floristic composition of a wasteland was determined under heterogeneous levels of trace
13 element contamination.
- 14 • Trace element contamination reduced biodiversity by selecting tolerant species.
- 15 • The dominant species, *Alliaria petiolata*, is a potential Zn bioindicator with the highest leaf Zn,
16 Ni and Cd uptake.
- 17 • Pb and As are the elements that presented the greatest risk to human health in the case of
18 accidental soil ingestion.

19

20

21

22 Abstract:

23

24

25 This study aimed to determine the trace element accumulation in the soil and plants in an industrial
26 wasteland and to estimate the extent of transfer to humans to measure the effects on and risks to
27 vegetation and human health and find bioindicator plants representative of the levels of the main
28 contaminants. In areas with the highest extractable trace element levels, we observed decreases in plant
29 biodiversity explained by the disappearance of several families, favouring the coverage of tolerant
30 species, such as *Urtica dioica* and *Hedera helix*. Trace elements were also found in the leaves of several
31 plants, especially in a dominant species that is poorly studied, *Alliaria petiolata*. Indeed, this species
32 had the highest contents of Zn (1750 mg.kg⁻¹ DW), Ni (13.1 mg.kg⁻¹ DW), and Cd (18 mg.kg⁻¹ DW)
33 found at the site and is a potential Zn bioindicator since its leaf contents were also representative of the
34 Zn extractable contents in soil ($R^2 = 0.94$). The hazard quotient and carcinogen risk revealed that most
35 of the site had an identified or possible risk, mainly due to Pb and As. Native species, especially *A.*
36 *petiolata*, could be used in phytoextraction to manage and limit these human and environmental risks.

37 Key words:

38 Industrial wasteland; *Alliaria petiolata*; Trace elements; Contaminated soils; Bioindicator; Human
39 health; Hazard quotient; Carcinogen risk; Phytomanagement.

40

41

42 **1 Introduction**

43 Due to human activities, large quantities of potentially toxic elements have been released into the
44 environment since the end of the 19th century (Zhang & Wang, 2020). These activities have led to the
45 formation of many marginal sites containing various organic and inorganic compounds in soil (Panagos
46 et al., 2013). The presence of these compounds may impair the ecosystem services provided by the soil
47 of these sites (Morel et al., 2015), such as provisioning services (raw materials, food) or regulating
48 services (water quality, carbon storage, maintaining biodiversity, Jónsson & Davíðsdóttir, 2016). The
49 cost of contamination management leads to a lack of interest in these sites and urban management that
50 favours the artificialization of agricultural land rather than the rehabilitation of these soils (Vidal-Baudet
51 & Rossignol, 2018). Approximately 690 000 industrial sites with past or current polluting activities were
52 identified in the European Union (EU) in 2018 (Paya Perez & Rodriguez Eugenio, 2018), while the
53 Géorisques database (<https://www.georisques.gouv.fr/>) listed 16 000 sites in France in 2022.
54 Contamination is due to various sources, such as industrial production and commercial services (36%),
55 the oil industry (17%), municipal waste (15%) and industrial waste (9%) (Paya Perez & Rodriguez
56 Eugenio, 2018). The most common contaminants affecting soil are trace elements (TEs) (Panagos et al.,
57 2013). Being nonbiodegradable, TEs tend to accumulate in the environment and could impact the
58 environment and human health (Ali et al., 2013), even at very low concentrations (Arora et al., 2008).

59 Most TEs are strongly bound to the soil; however, there is always a spreading risk due to the mobile
60 fraction that can be transferred into the ecosystem (Qasim & Motelica-Heino, 2014). Moreover, if some
61 TEs, such as Zn, Cu or Mn, are essential for the health and development of plants and animals (Alloway,
62 2013), excessive contents may have adverse impacts. Some other TEs without known biological
63 function (e.g., Cd, Pb) present high toxicity for most organisms. The effect of TEs depends on their
64 contents and physico-chemical properties, Zn, Pb, Cd, Cu and Ni being frequently studied elements, as
65 they are considered to have the greatest impact on organisms (Diatta et al., 2003). They can provoke
66 damage to cells (Kabata-Pendias, 2011) and disrupt cellular processes such as photosynthesis among
67 primary producers (Prasad & Strzałka, 1999; Warsi et al., 2023), cause oxidative stress, generate

68 neurotoxic effects, disrupt the function of numerous enzymes, and increase cancer risk (Ali et al., 2013;
69 Turdi & Yang, 2016).

70 As primary producers, plants are some of the first organisms to suffer from high TE contents in soils.
71 TE transfer from soil to plants constitutes crucial information for understanding the environmental
72 impacts of these pollutants. Ions enter plants through their roots and are then either directly stored or
73 translocated to the shoots through xylem vessels and more specifically deposited in vacuoles
74 (Verbruggen et al., 2009; Rascio & Navari-Izzo, 2011). Sequestration in vacuoles is a way to cope with
75 high metal concentrations and limit their impact on metabolic processes, increasing plant tolerance to
76 TE-contaminated soils (Jabeen et al., 2009). In this way, TEs could be transferred into food chains and
77 will accumulate through networks to become potentially harmful for plant and animal health, including
78 that of humans (Aycicek et al., 2008; Rajaganapathy et al., 2011).

79 In the context of the rehabilitation of industrial territories, it is necessary to manage marginal sites, often
80 localized around urban areas, to restore their value, in particular through ecosystem services and hence
81 the development of new uses. Proper management of soil pollution requires knowledge of the risks and
82 impacts of contaminants on human health and the environment. For this purpose, plants can be vectors
83 of information about the contamination degree and toxic effects (Diatta et al., 2003). The capacity of a
84 plant to be used as a bioindicator mostly depends on its capacity to take up and accumulate contaminants
85 to a level representative of soil contents (Kabata-Pendias, 2011; Favas et al., 2012). The risk for human
86 health associated with exposure to contaminants can be assessed by measuring the hazard quotient (HQ)
87 and carcinogenic risks (CR) according to scenarios of human ingestion of soil and/or plants from a
88 contaminated site (Antoine et al., 2017; Dehghani et al., 2018). These indexes provide information about
89 the human risk associated with each contaminant present at a site and therefore about the management
90 priorities for the elements present.

91 In this context, the aims of the present study are as follows: i) Locate and quantify TEs in soil and
92 determine their effect on the floristic diversity of an industrial wasteland. This diversity will be assessed
93 by a floristic survey as well as the measurement of the vegetation cover of species. ii) Determine the
94 accumulation of TEs in plants to estimate the potential of using indigenous plants as bioindicators of

95 contamination as well as measuring the TE effect on nutrient accumulation. For this purpose, the leaf
96 contents of TEs and their relationship with the soil contents will be measured. iii) Calculate the human
97 HQ and CR for individuals exposed to contaminants by soil ingestion and consumption of edible plants.
98 Contaminant levels in soil and plant leaves will be used for the calculation based on the elemental
99 toxicity and exposure scenarios.

100 We hypothesized that the variable level of TEs on the site induced the presence of different plant
101 communities by reducing biodiversity and selecting tolerant species in heavily contaminated areas. TEs
102 can also have toxic effects on plants and pose a risk for human health in the event of exposure. On the
103 other hand, among the tolerant species at the site, some could be bioindicators with potential to be used
104 in management decisions.

105

106 **2 Materials and methods**

107 **2.1 Study site**

108 The study site is a 2 ha industrial wasteland located in the city of Vieux-Charmont (47°31'15.8"N,
109 6°50'23.8"E) in eastern France. This wasteland is surrounded by dwellings, a pond created in 1957, the
110 river “La savoureuse” and 2 operational factories (Fig. 1). Several activities have taken place in the
111 factories since 1871, such as watchmaking, heat treatment and manufacture of piston pins, cars and
112 precision parts. The site was used as an uncontrolled landfill for industrial and household wastes, found
113 buried and on the surface. The wasteland was closed to the public in 2007 after soil analysis revealed
114 contamination by organic (PAH, PCB) and inorganic (Zn, Pb, Cd, As, Cu, Ni, Cr, Hg) compounds.



115

116 *Fig. 1. The industrial wasteland of Vieux-Charmont (Doubs, France). (A) Location of the Vieux-Charmont wasteland (in red)*
117 *and its environment. (B) Aerial picture of the Vieux-Charmont wasteland entrance. (C) Aerial picture of the Vieux-Charmont*
118 *wasteland and its environment.*

119 **2.2 Floristic survey**

120 From June to July 2020, a floristic survey of the herbaceous layer was carried out in 8 zones; 4 zones
121 had intense woody cover and were named undergrowth zones (UZ, zones 1 to 4), and 4 zones were

122 considered open zones (OZ, zones 5 to 8) with low woody cover, as representative as possible of the
123 diversity of the accessible parts of the site (Fig. S1). Each zone was homogenous in terms of vegetation,
124 cover, stratification and human intervention. Between 10 and 20 quadrats of 0.2 m² were randomly
125 delimited on each zone, and the species present on these surfaces were determined as well as their cover
126 value based on the Braun-Blanquet scale and cover estimation (+, 1, 2, 3, 4, 5 for 0.1, 2.5, 15, 37.5, 62.5,
127 87.5%, respectively) (Wikum & Shanholtzer, 1978; Anne et al., 2021). Based on these data, four
128 diversity indices were calculated: species richness, Shannon index (eq. 1), Simpson index (eq. 2) and
129 Hill index (eq. 3).

$$130 \quad H' = - \sum (p_i \cdot \log(p_i)) \quad (\text{eq. 1})$$

$$131 \quad \lambda = 1 - (\sum(p_i^2)) \quad (\text{eq. 2})$$

$$132 \quad \text{Hill} = 1 - \left(\frac{\lambda - 1}{\exp(H')} \right) \quad (\text{eq. 3})$$

133 p_i being the cover value of species i divided by the total plant cover value. The Simpson and Hill indices
134 are subtracted from 1; thus, for each of the four indices, an increase in value means higher diversity.

135 2.3 Soil sampling and analyses

136 In May 2021, soil was sampled in 125 zones (10 m x 10 m) that cover all accessible parts of the site
137 (Fig. S1). A composite sample was collected in each zone by mixing 4 samples taken from the corners
138 and 1 sample taken in the middle of the zone at a depth of 0-30 cm. The samples were then stored in
139 plastic bags and air dried before analysis. The pH value was determined directly on the soil samples
140 using a field Soil Stick pH meter (Spectrum Technologies, Inc., Aurora, USA) (Tano et al., 2020). The
141 total element content was measured on a 500 mg dry soil sample using inductively coupled plasma
142 atomic emission spectrometry (ICP–AES, Thermo Fischer Scientific, Inc., Waltham, USA) after acid
143 digestion (DigiPREP system, SCP Sciences, Courtaboeuf, France) using a mixture of 2 ml of 67% nitric
144 acid, 6 ml of 34% hydrochloric acid and 2 ml of 48% hydrofluoric acid (Ciadamidaro et al., 2019).

145 Soil samples collected for total element fraction measurements were also used to ensure at least 3
146 measurements of the extractable fraction in each floristic survey zone (the number of samples depended

147 on the surface). These samples are related to one of the 125 zones described in Fig. S1 and are considered
148 representative of the zone. 2.5 g of dried soil was extracted with 25 ml of 0.01 M CaCl₂ solution under
149 constant agitation at 100 rpm for 3 h (Houba et al., 1996). Then, the samples were filtered, acidified at
150 1% (v/v) and quantified by ICP–AES.

151 2.4 Plant sampling

152 Leaf samples were collected from the genera *Acer*, *Ailanthus*, *Alliaria* (on first- or second-year plants),
153 *Betula*, *Fraxinus*, *Glechoma*, *Populus*, *Prunus*, *Quercus*, *Salix* and *Urtica*, which are well represented
154 herbaceous plants, shrubs and trees found throughout the site during two campaigns in summer 2018
155 and autumn 2021. A maximum of one sample per species was sampled in the 125 zones previously
156 described (Fig. S1). The samples were stored in plastic bags at 4°C until washing with distilled water to
157 remove soil particles. Samples were then dried in an oven at 70°C and crushed for 3 min in a mixer mill
158 (MM 200, Retsch, Éragny, France) at 30 rps before analysis. The plant element concentration was
159 measured in 100 mg samples using ICP–AES after acid digestion using a mixture of 2 ml of 67% nitric
160 acid and 0.5 ml of 35% oxygen peroxide (Assad et al., 2017).

161 2.5 Measurement of the human health risk

162 Based on the contaminant contents in the total soil fraction and in edible plant leaves, the daily intake
163 (DI; eq. 4) of contaminants was calculated according to the French national methodology of
164 management of polluted sites and soils (MEEM, 2017). Two exposure scenarios were considered in the
165 present study: (1) ingestion of 91 mg of soil per day (Stanek et al., 2001) while frequenting the site 148
166 days a year for 6 years by a 15 kg child and (2) ingestion of 37.5 g of edible plant leaves per day
167 (Barbillon et al., 2019), 26 days a year, corresponding to 7% of the total leaf consumption from the site,
168 for 6 years by a 15 kg child. Two plants with edible leaves are considered, *Alliaria petiolata* and *Urtica*
169 *dioica*.

$$170 \quad DI \text{ (mg.kg}^{-1}.\text{day}^{-1}) = \frac{C \times IR \times EF \times ED}{BW \times (AT \times 365)} \quad (\text{eq. 4})$$

171 C is the concentration of the material ingested (mg.kg⁻¹ of dry weight for soil and mg.kg⁻¹ of fresh weight
172 for leaves); IR is the intake rate of material (kg.day⁻¹); EF is the exposure frequency (day.year⁻¹); ED is

173 the exposure duration (years); BW is the body weight (kg); AT is the average time (years), equivalent
174 to ED for noncarcinogenic contaminants or a lifetime (70 years) for carcinogenic contaminants (MEEM,
175 2017).

176 The hazard quotient (HQ; eq. 5) for threshold effects and the carcinogenic risk (CR; eq. 6) for non-
177 threshold effects were calculated for each contaminant studied when the toxicological reference value
178 (TRV) was available (As, Cd, Cr, Cu, Hg, Ni, Pb and Zn for threshold effects and As, Cr and Pb for
179 non-threshold effects). In accordance with the national methodology (MEEM, 2017), the DI values were
180 compared to TRV, as described in Table S1.

$$181 \quad HQ = \frac{DI}{TRV} \quad (eq. 5)$$

$$182 \quad CR = DI \times TRV \quad (eq. 6)$$

183 For HQ and CR, the sum of the values for the soil and plant scenarios in each soil sampling area are
184 considered for interpretation. According to the methodology, there is no risk for HQ values < 0.2 and
185 CR values < 10⁻⁶, a possible risk for HQ values between 0.2 and 5 and CR values between 10⁻⁶ and 10⁻⁴
186 and an identified risk for HQ values ≥ 5 and CR values ≥ 10⁻⁴ (MEEM, 2017).

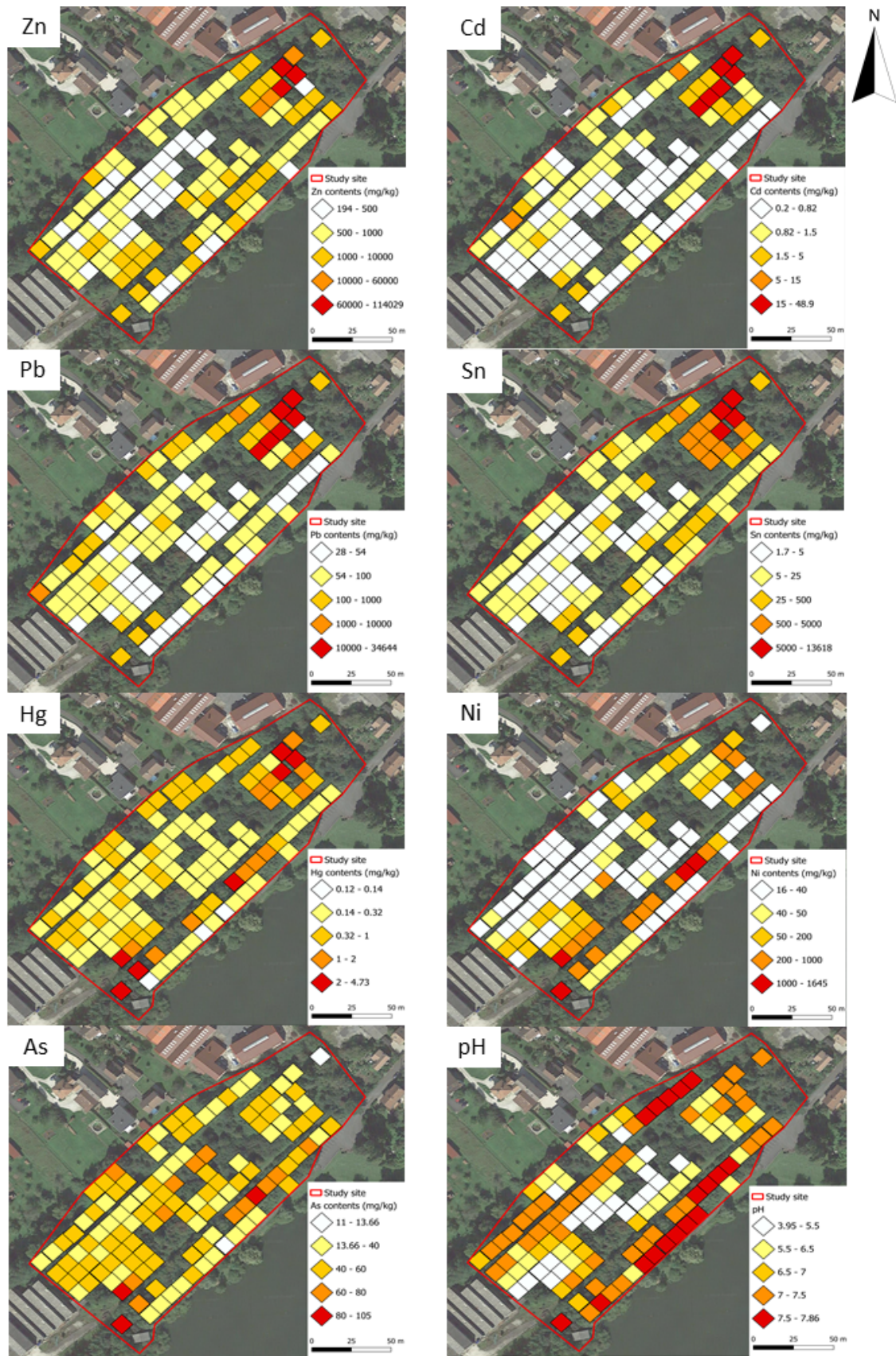
187 2.6 Mapping and statistical analysis

188 Mapping was performed with QGIS (ver. 3.16) using Google background maps. The analyses were
189 performed using R (ver. 4.1.1) with the packages *agricolae* (De Mendiburu, 2021), *corrplot* (Wei &
190 Simko, 2021), *cowplot* (Wilke, 2020), *ggplot2* (Wickam, 2016), *Hmisc* (Harrell, 2022), and *vegan*
191 (Oksanen et al., 2022). For all the tests performed, results were considered statistically significant at a p
192 value < 0.05. The Shannon and Simpson diversity indices were calculated using *vegan*. The normality
193 of the data was first tested using Shapiro–Wilk and Levene tests. Comparisons of means were made
194 using Kruskal–Wallis tests for biodiversity indices and extractable TE contents by vegetation zone as
195 well as for foliar TE contents between genera. Spearman’s test was used to assess the correlation
196 between biodiversity indices and TE extractable contents, between pH values and TE extractable
197 percentage and between soil total contents of TEs and nutrient contents in plant leaves. The graphs were
198 made using the *ggplot2* package, and the correlation matrix was made using the *corrplot* package.

199 3 Results

200 3.1 Soil TE contents

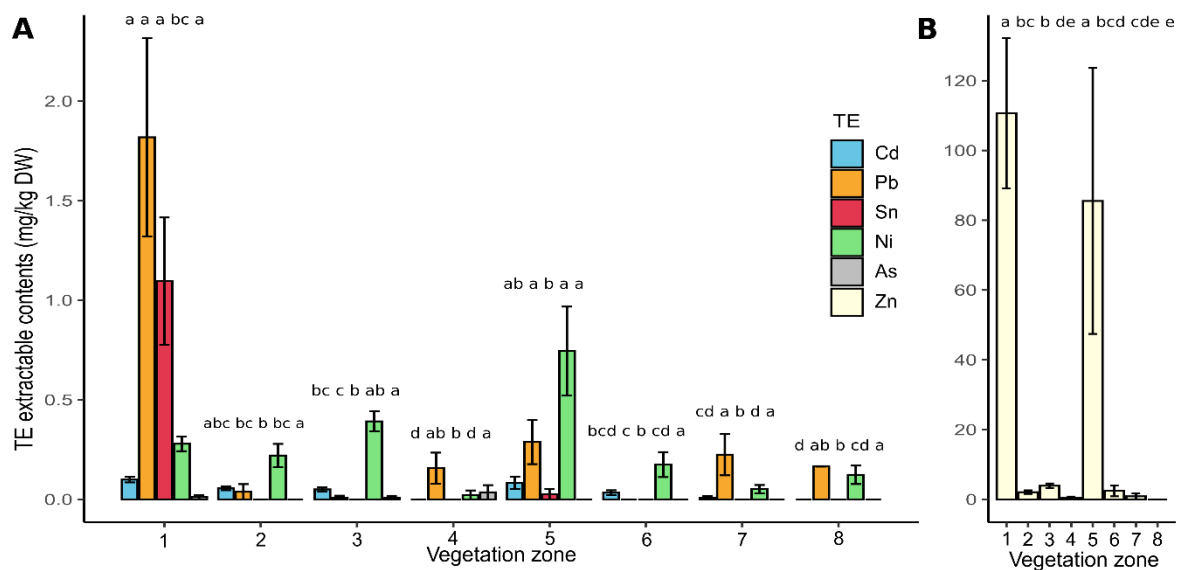
201 The main contaminants found at the site were Zn, Pb, Cd, Sn, Hg, Ni and As (Fig. 2), which were
202 heterogeneously distributed throughout the investigated area. Indeed, in most of the wasteland, the
203 measured contents varied from 200 to 10 000 mg.kg⁻¹ dry weight (DW) for Zn, 0.2 to 10 mg.kg⁻¹ DW
204 for Cd, 30 to 2 500 mg.kg⁻¹ DW for Pb, 2 to 1 830 mg.kg⁻¹ DW for Sn and 0.12 to 2 mg.kg⁻¹ DW for
205 Hg. However, the contaminant map highlighted a heavily contaminated zone of almost 500 m² in the
206 northeast of the site that contained the highest amounts of Zn (36 000–115 000 mg.kg⁻¹ DW), Pb
207 (13 500–34 600 mg.kg⁻¹ DW), Cd (17–50 mg.kg⁻¹ DW), Sn (3 200–13 600 mg.kg⁻¹ DW), and Hg (1.4–
208 4.5 mg.kg⁻¹ DW). Concerning Ni and As, the contents varied from 16 to 1650 mg.kg⁻¹ DW and 11 to
209 105 mg.kg⁻¹ DW, respectively. The highest contents for these two elements were localized in the south
210 of the site, close to the factory and the pond. In addition, the site was also contaminated with Cr (26-
211 1475 mg.kg⁻¹ DW), Cu (24–1800 mg.kg⁻¹ DW), Fe (13 000–224 000 mg.kg⁻¹ DW) and Mn (250–2300
212 mg.kg⁻¹ DW). Cu was localized in the most contaminated area of the site (northeast), and Cr, Fe and Mn
213 were localized in the southern part of the site, similar to Ni and As. The pH values were heterogeneous
214 throughout the site, although they remained close to neutral, with values that varied from 6.4 to 7.3 in
215 the most contaminated zone (Fig. 2). The other part of the site had pH values that varied from 4 to 7.9,
216 and the lowest pH value (4–5.5) was localized along a line from the southwest of the site to the centre.



217

218 *Fig. 2. Maps of total contents of the main contaminants (Zn, Cd, Pb, Sn, Hg, Ni, As) and pH value localized at the soil sampling*
 219 *plots described in Fig. S1 in the industrial wasteland. For TE contents, the first levels of the scale (white square) range from*
 220 *the minimum values found on the site to twice the world soil average values defined by Kabata-Pendias (2011), except for Zn,*
 221 *where the minimum value was too high.*

222 The analysis of the bioavailable fractions further revealed this high heterogeneity for both the UZ (zones
 223 1 to 4) and OZ (zones 5 to 8) (Fig. S1 & 3). Zones 1 and 5 were statistically the most contaminated
 224 zones, with Zn extractable contents of 110 and 85 mg.kg⁻¹ DW, respectively, while the other zones had
 225 Zn contents of < 4 mg.kg⁻¹ DW (Fig. 3B). Furthermore, the same distribution was observed in zone 1
 226 for Sn, with a mean value of 1.1 mg.kg⁻¹ DW; this value was higher than that in the other zones, with a
 227 content of 0.026 in zone 5 and contents below the limits of quantification (< LQ) in the other zones.
 228 Zone 5 had the highest contents of Ni, with a value of 0.74 mg.kg⁻¹ DW, which was statistically higher
 229 than that in the other zones (except zone 3), where the contents were in the range of 0.02-0.39 mg.kg⁻¹
 230 DW. For other TEs, although zones 1 and 5 had the highest Pb and Cd contents, the differences in
 231 content were lower. Indeed, the contents varied from 0.01 to 0.1 mg.kg⁻¹ DW for Cd (< LQ for zones 4
 232 and 8), from 0.01 to 1.8 mg.kg⁻¹ DW for Pb (< LQ for zone 6) and from 0.01 to 0.036 mg.kg⁻¹ DW for
 233 As (< LQ for zones 2, 5, 6, 7 and 8) (Fig. 3A).



234

235 *Fig. 3. Mean CaCl₂ extractable contents (mg.kg⁻¹ DW) of Cd, Pb, Sn, Ni, As (A) and Zn (B) in the 8 floristic survey zones and*
 236 *standard errors. Letters in common indicate statistically similar groups at p < 0.05 according to Kruskal-Wallis and post hoc*
 237 *pairwise comparison tests.*

238 3.2 Plant diversity

239 The floristic survey, conducted over a total area of 4860 m², and the vegetation samples led to the
 240 identification of 96 species (including 72 herbaceous species) belonging to 40 families (Tables 1 & 2).

241

242 Table 1. Identification and frequency of species from the herbaceous layer on the Vieux-Charmont wasteland. Frequencies
 243 were measured based on the number of quadrats in the floristic survey.

Family	Species	Frequency	Family	Species	Frequency
Aceraceae	<i>Acer campestre</i>	23.6	Juglandaceae	<i>Juglans regia</i>	0.9
Aceraceae	<i>Acer pseudoplatanus</i>	4.5	Lamiaceae	<i>Galeopsis tetrahit</i>	21.8
Adoxaceae	<i>Sambucus nigra</i>	15.5	Lamiaceae	<i>Glechoma hederacea</i>	29.1
Apiaceae	<i>Aethusa cynapium</i>	1.8	Lamiaceae	<i>Lamium maculatum</i>	10.0
Apiaceae	<i>Daucus carota</i>	8.2	Lamiaceae	<i>Stachys sylvatica</i>	0.9
Apiaceae	<i>Heracleum sphondylium</i>	1.8	Malvaceae	<i>Malva moschata</i>	1.8
Apiaceae	<i>Torilis japonica</i>	8.2	Malvaceae	<i>Malva alcea</i>	0.9
Aquifoliaceae	<i>Ilex aquifolium</i>	1.8	Oxalidaceae	<i>Oxalis stricta</i>	2.7
Araliaceae	<i>Hedera helix</i>	42.7	Papaveraceae	<i>Chelidonium majus</i>	0.9
Asteraceae	<i>Achillea millefolium</i>	4.5	Plantaginaceae	<i>Linaria vulgaris</i>	8.2
Asteraceae	<i>Artemisia vulgaris</i>	3.6	Plantaginaceae	<i>Plantago lanceolata</i>	0.9
Asteraceae	<i>Cirsium arvense</i>	1.8	Poaceae	<i>Agrostis capillaris</i>	14.5
Asteraceae	<i>Cirsium vulgare</i>	3.6	Poaceae	<i>Arrhenaterum elatius</i>	12.7
Asteraceae	<i>Crepis capillaris</i>	6.4	Poaceae	<i>Avena fatua</i>	2.7
Asteraceae	<i>Erigeron annuus</i>	26.4	Poaceae	<i>Brachypodium sylvaticum</i>	0.9
Asteraceae	<i>Erigeron canadensis</i>	6.4	Poaceae	<i>Dactylis glomerata</i>	19.1
Asteraceae	<i>Jacobea vulgaris</i>	2.7	Poaceae	<i>Elymus caninus</i>	4.5
Asteraceae	<i>Lactuca serriola</i>	3.6	Poaceae	<i>Elystrigia repens</i>	1.8
Asteraceae	<i>Lapsana communis</i>	5.5	Poaceae	<i>Holcus lanatus</i>	6.4
Asteraceae	<i>Picris hieracioides</i>	0.9	Poaceae	<i>Poa trivialis</i>	9.1
Asteraceae	<i>Tanacetum vulgare</i>	8.2	Poaceae	<i>Triticum aestivum</i>	3.6
Asteraceae	<i>Tripleurospermum inodorum</i>	1.8	Polygonaceae	<i>Reynoutria japonica</i>	0.9
Berberidaceae	<i>Berberis aquifolium</i>	1.8	Rosaceae	<i>Crataegus monogyna</i>	20.9
Brassicaceae	<i>Alliaria petiolata</i>	40.9	Rosaceae	<i>Crataegus laevigata</i>	8.2
Campanulaceae	<i>Campanula patula</i>	6.4	Rosaceae	<i>Geum urbanum</i>	8.2
Cannabaceae	<i>Humulus lupulus</i>	0.9	Rosaceae	<i>Potentilla reptans</i>	2.7
Caprifoliaceae	<i>Dipsacus fullonum</i>	0.9	Rosaceae	<i>Prunus avium</i>	1.8
Caryophyllaceae	<i>Silene vulgaris</i>	0.9	Rosaceae	<i>Prunus spinosa</i>	4.5
Convolvulaceae	<i>Convolvulus sepium</i>	5.5	Rosaceae	<i>Prunus domestica</i>	2.7
Cornaceae	<i>Cornus sanguinea</i>	7.3	Rosaceae	<i>Rubus fruticosus</i>	54.5
Dryopteridaceae	<i>Dryopteris filix-mas</i>	1.8	Rosaceae	<i>Rubus caesius</i>	5.5
Euphorbiaceae	<i>Euphorbia dulcis</i>	8.2	Rubiaceae	<i>Galium aparine</i>	23.6
Fabaceae	<i>Lathyrus pratensis</i>	0.9	Rubiaceae	<i>Galium mollugo</i>	18.2
Fabaceae	<i>Melilotus albus</i>	6.4	Rubiaceae	<i>Galium rotundifolium</i>	0.9
Fabaceae	<i>Robinia pseudoacacia</i>	2.7	Rubiaceae	<i>Galium palustre</i>	11.8
Fabaceae	<i>Trifolium pratense</i>	4.5	Scrophulariaceae	<i>Verbascum blattaria</i>	0.9
Fabaceae	<i>Vicia cracca</i>	2.7	Simaroubaceae	<i>Ailanthus altissima</i>	6.4
Fabaceae	<i>Vicia sepium</i>	0.9	Solanaceae	<i>Solanum nigrum</i>	0.9
Fagaceae	<i>Quercus robur</i>	0.9	Taxaceae	<i>Taxus baccata</i>	1.8
Geraniaceae	<i>Geranium robertianum</i>	4.5	Urticaceae	<i>Urtica dioica</i>	24.5
Geraniaceae	<i>Geranium pusillum</i>	0.9	Verbenaceae	<i>Verbena officinalis</i>	2.7
Hypericaceae	<i>Hypericum humifusum</i>	0.9	Vitaceae	<i>Parthenocissus quinquefolia</i>	3.6
Hypericaceae	<i>Hypericum perforatum</i>	14.5			

244

245

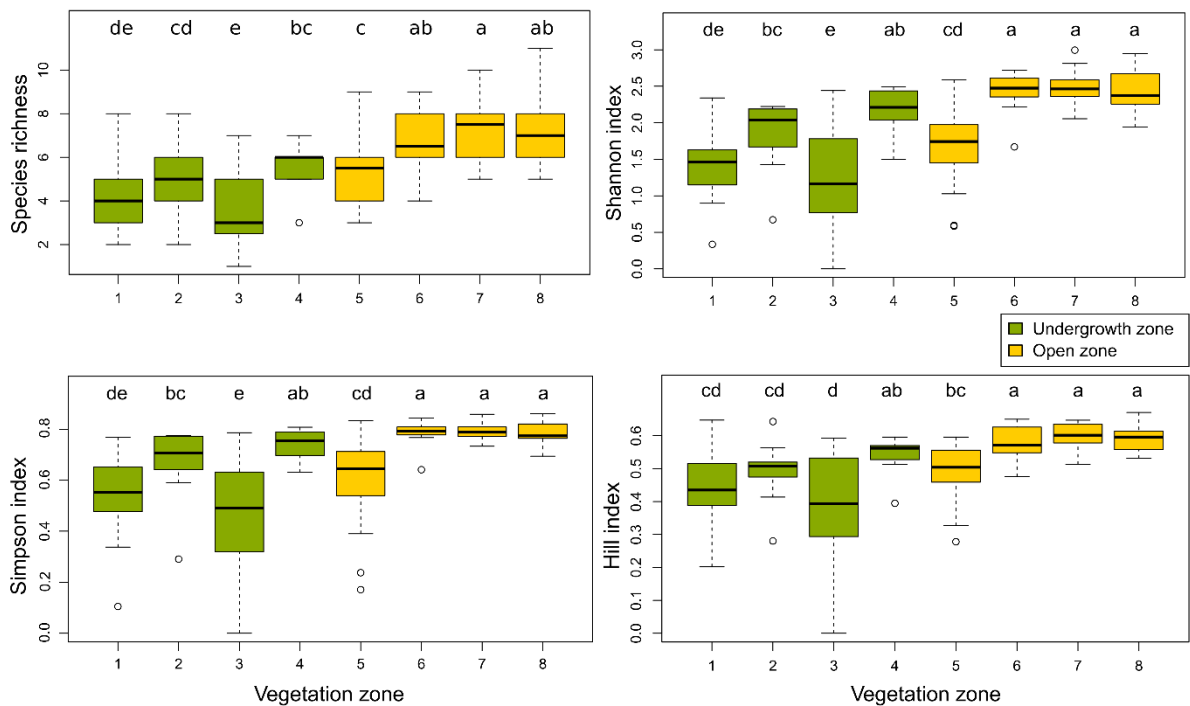
246

247 Table 2. Shrubs and tree species identified by leaf sampling on the Vieux-Charmont wasteland. Frequencies were measured
 248 based on the 125 zones used for soil and plant samplings.

Family	Species	Frequency (%)
Betulaceae	<i>Betula verrucosa</i>	0.8
Fagaceae	<i>Quercus petraea</i>	2.4
Malvaceae	<i>Tilia platyphyllos</i>	0.8
Oleaceae	<i>Fraxinus excelsior</i>	4
Rosaceae	<i>Prunus serotina</i>	0.8
Salicaceae	<i>Populus nigra</i>	0.8
Salicaceae	<i>Populus tremula</i>	3.2
Salicaceae	<i>Salix alba</i>	0.8
Salicaceae	<i>Salix fragilis</i>	1.6
Salicaceae	<i>Salix purpurea</i>	4
Salicaceae	<i>Salix viminalis</i>	0.8

249
 250 The main families of surveyed species were Asteraceae, Poaceae and Fabaceae (13, 10 and 5 species,
 251 respectively), which represented almost 40% of the herbaceous species, as well as Salicaceae and
 252 Rosaceae (6 species each), which represented 50% of shrubs and tree species. However, some families
 253 were also well represented due to the frequency of certain member species. Indeed, *Hedera helix* was
 254 the only species observed from the Araliaceae family, but its frequency was 42.7%. Similarly, the
 255 Brassicaceae family was exclusively represented by *A. petiolata* with a frequency of 40.9%. These two
 256 plants, along with the Rosaceae species *Rubus fruticosus* (frequency of 54.5%), were the most frequent
 257 herbaceous species on the site. Conversely, 25 species were observed only once and had a frequency of
 258 less than 1%, such as the herbaceous species *Dipsacus fullonum* (Caprifoliaceae), *Hypericum humifusum*
 259 (Hypericaceae) and *Verbascum blattaria* (Scrophulariaceae) and the tree species *Tilia platyphyllos*
 260 (Malvaceae), *Prunus serotina* (Rosaceae) and *Salix alba* (Salicaceae).

261 The species richness ranged from 3.7 to 5.6 in the UZ (zones 1 to 4) and from 5.4 to 7.4 in the OZ (zones
 262 5 to 8); the Shannon index, from 1.17 to 2.09 in the UZ and from 1.61 to 2.39 in the OZ; the Simpson
 263 index, from 0.44 to 0.72 in the UZ and from 0.58 to 0.77 in the OZ; and the hill index, from 0.38 to 0.54
 264 in the UZ and from 0.48 to 0.59 in the OZ (Fig. 4).

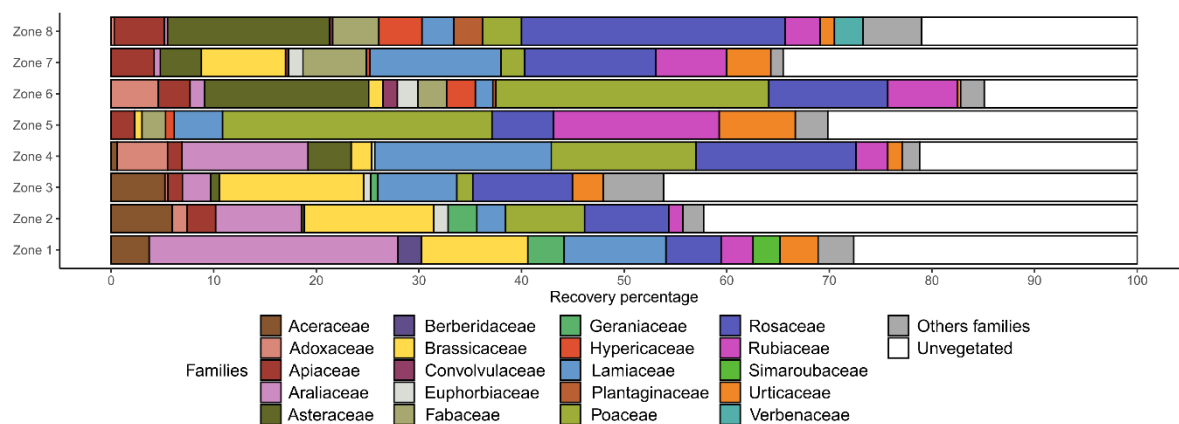


265

266 *Fig. 4. Boxplots of Shannon, Simpson and Hill indices and species richness in the 0.2 m² quadrats of the 8 survey zones. Letters*
 267 *in common indicate statistically similar groups at p < 0.05 according to Kruskal–Wallis and post hoc pairwise comparison*
 268 *tests.*

269 Overall, the OZ had statistically higher biodiversity indices than the UZ (p values < 0.01), except for
 270 zone 4, which was the least contaminated part of the UZ, and zone 5, which was the most contaminated
 271 part of the OZ. We also observed that the biodiversity indices of zone 4 were all statistically higher than
 272 those of zones 1 and 3. This was also the case for zone 2 but only for the Shannon and Simpson indices.
 273 Concerning the OZ, the most contaminated area (zone 5) had a systematically lower biodiversity for
 274 each index than the three other zones. In addition, the TE extractable contents and the biodiversity
 275 indices for the UZ had significant anticorrelations with Zn (from -0.28 to -0.45) and Ni (from -0.39 to -
 276 0.57). For the OZ, there were not only anticorrelations with Zn (from -0.44 to -0.6) and Ni (from -0.48
 277 to -0.62) but also with Cd (from -0.44 to -0.6), Pb (from -0.36 to -0.61) and Sn (from -0.47 to -0.68).

278 In addition to these relationships between biodiversity and TE extractable contents, the plant
 279 communities also differed from one zone to another (Fig. 5). Indeed, in the UZ, the Adoxaceae,
 280 Apiaceae, Asteraceae, Euphorbiaceae and Poaceae families appeared in zones 2, 3 and 4 but not in zone
 281 1, which was the most contaminated. Moreover, the Rosaceae family represented almost 5.4% of the
 282 plants in zone 1, unlike the other zones, where it represented between 8.2 and 15.6%.



283

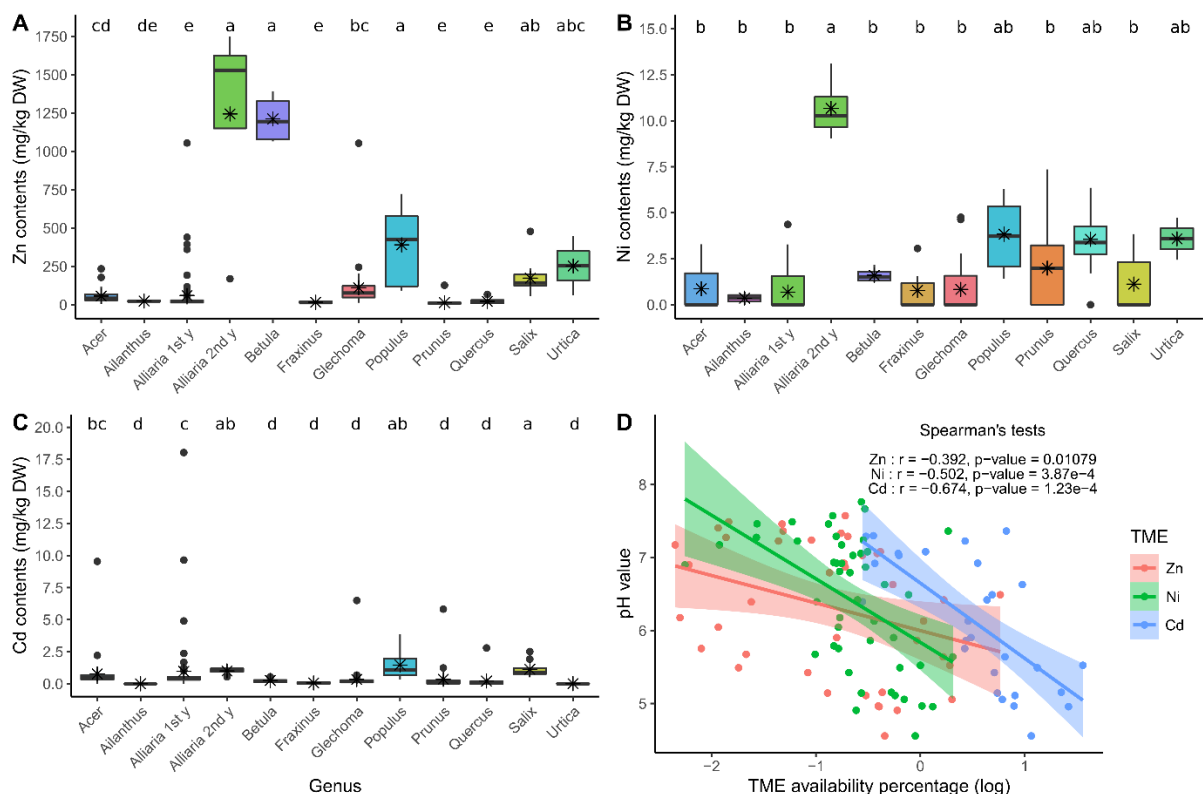
284 Fig. 5. Plant communities present in the floristic survey zones expressed as a recovery percentage of the 37 families identified
 285 and unvegetated parts.

286 In contrast, Berberidaceae and Simaroubaceae, each represented by only one species at the site, *Ilex*
 287 *aquifolium* and *Ailanthus altissima*, respectively, were found only in zone 1. The Araliaceae family, also
 288 represented by only one species, *H. helix*, represented a quarter of the vegetation (24.25%) in zone 1,
 289 while it represented 2.75 to 12.3% of the vegetation in other areas. Concerning the OZ, Asteraceae and
 290 Convolvulaceae were not found in the most contaminated zone (zone 5) but were present in the other
 291 zones. The Rosaceae family was also less represented in the most contaminated area, with a cover
 292 percentage of 6%, compared with 11.6 to 25.7% for the other zones. Conversely, Rubiaceae and
 293 Urticaceae were more represented in zone 5, accounting for 16.15 and 7.4% of the vegetation,
 294 respectively, in comparison to other zones, where the values varied from 3.4 and 6.9 for Rubiaceae and
 295 from 0.3 to 4.3 for Urticaceae. Globally, except for the most contaminated zones (zones 1 and 5), the
 296 families identified were similar between the UZ (except Geraniaceae in zone 4 and Urticaceae in zone
 297 2) and the OZ (except Adoxaceae and Plantaginaceae in zone 7 and Euphorbiaceae and Verbenaceae in
 298 zone 8).

299 3.3 TE uptake by the vegetation

300 *A. petiolata* was the plant species with the highest maximal Zn, Ni and Cd contents, with 1750, 13.1 and
 301 18 mg.kg⁻¹ DW, respectively (Fig. 6). The data also highlighted that the second-year *A. petiolata*
 302 accumulated significantly more of these TEs than the first-year plants. For Cd, the maximal content
 303 value was found in first-year plants. The Zn, Ni and Cd contents in leaves were highly dependent on the

304 plant genus considered. Indeed, *Alliaria* (second-year plants), *Betula*, *Populus*, *Salix*, *Glechoma* and
 305 *Urtica* contained an average of 1250, 1210, 390, 174, 111 and 253 mg.kg⁻¹ DW of Zn, respectively.
 306 Those values were significantly higher than those for the *Ailanthus*, *Alliaria* (first-year plants), *Fraxinus*,
 307 *Prunus* and *Quercus* genera, where the contents were between 13 and 60 mg.kg⁻¹ DW. For Ni, second-
 308 year *Alliaria* had a mean content of 10.7 mg.kg⁻¹ DW, which was statistically higher than that of the
 309 other plant genera (except *Populus*, *Quercus* and *Urtica*), where the values varied from 0.36 to 2 mg.kg⁻¹
 310 ¹ DW. Concerning Cd, *Alliaria* (second-year plants), *Populus* and *Salix* had mean contents of 1.00, 1.46
 311 and 1.13 mg.kg⁻¹ DW, respectively, which were statistically higher than those of other genera (except
 312 *Acer*), where the values were between 0.09 and 0.96 mg.kg⁻¹ (< LQ for *Ailanthus* and *Urtica*). The data
 313 also showed high Mn contents in the leaves of *Quercus* and *Acer* species, with an average of 400 (max
 314 = 1 350) and 280 mg.kg⁻¹ (max = 2 400), respectively. In contrast, other genera showed mean Mn
 315 contents that varied from 15 to 150 mg.kg⁻¹ with a maximal value of 550 mg.kg⁻¹.

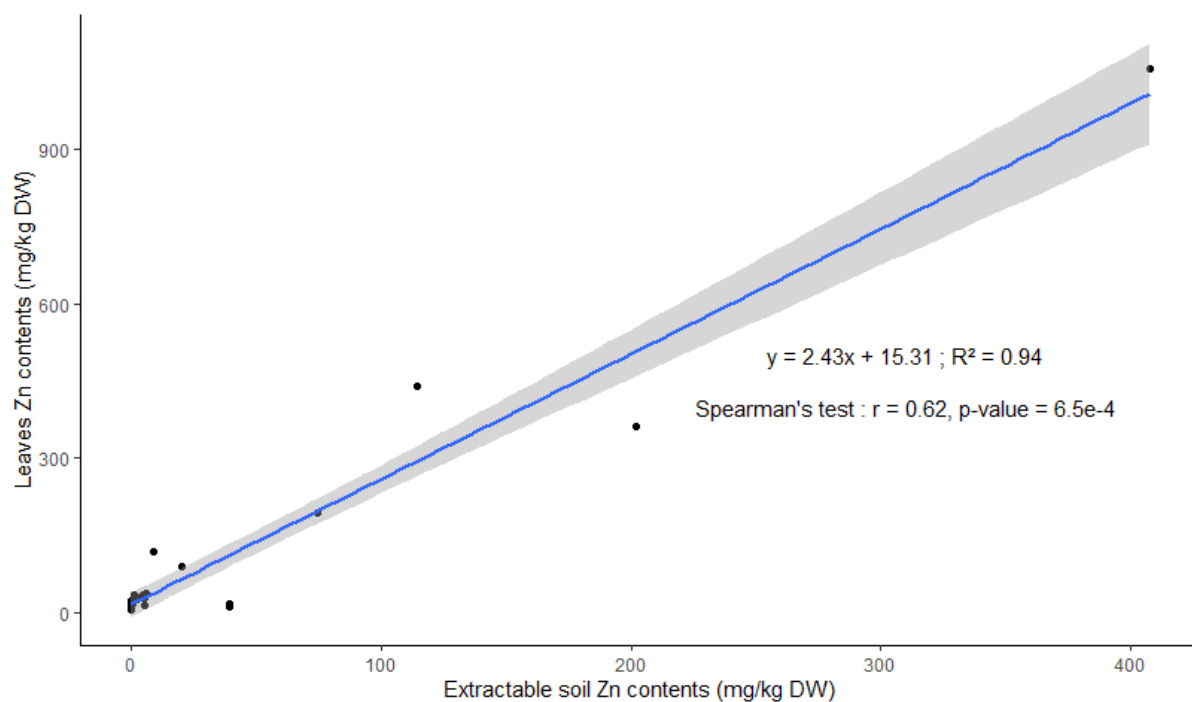


316

317 *Fig. 6. Leaf contents of Zn (A), Ni (B) and Cd (C) in the main plant genera and TE CaCl₂ extractable percentage as a function*
 318 *of pH value (D). The mean value of TE contents in each plant genera is represented by stars in the boxplots. Samples from*
 319 *first-year plants (1st y) and second-year plants (2nd y) are separated for the Alliaria genus. The TE availability is expressed*
 320 *as a logarithm of the percentage of TE availability (extractable contents of TE divided by total contents of TE). The 95%*
 321 *confidence interval is represented in a scatter plot around the equation lines.*

322 The mean Fe and Cu contents in leaves were 82 mg.kg⁻¹ DW (max = 370) and 7 mg.kg⁻¹ DW (max =
323 42), respectively, for all the genera. Finally, for As, Pb, Cr, Hg and Sn contents in plant leaves, most of
324 the samples had values < LQ. However, the data still showed that Pb reached 10.7 mg.kg⁻¹ DW and As
325 reached 4.2 mg.kg⁻¹ DW for *Alliaria*. We also showed that pH values were anticorrelated with Zn, Ni
326 and Cd availability percentages (Fig. 6), indicating that the extractable contents increased with
327 decreasing pH values. We also highlighted that the anticorrelation was highest for Cd (r = -0.67),
328 followed by Ni (r = -0.5) and finally Zn (r = -0.39). No correlations were found between the pH and the
329 available percentages of As, Pb and Sn.

330 In addition to the high contaminant contents found in *A. petiolata*, the data showed that Zn leaf contents
331 in first-year plants were representative of soil extractable Zn contents. Indeed, as highlighted in Fig. 7,
332 the scatter plot of these two parameters showed that the leaf contents were strongly related to the
333 extractable contents since the R² value of the relationship was 0.94. Furthermore, there was a positive
334 correlation between these two parameters with an r value of 0.62. This link was observed only for first-
335 year plants.

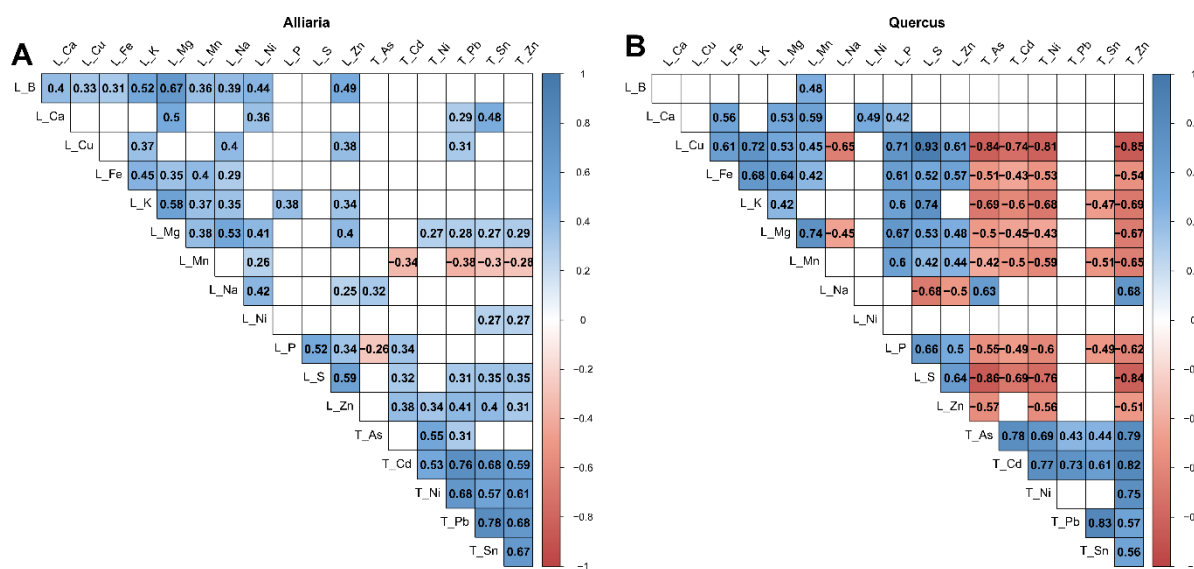


336

337 Fig. 7. Scatter plot of the first-year *Alliaria petiolata* Zn leaf contents depending on Zn CaCl₂ extractable contents of soil and
338 Spearman correlation test between these two parameters. The 95% confidence interval is represented around the relationship.

339 3.4 TE toxicity and risk assessment for plants and humans

340 The correlations between the nutrient contents in leaves and the TE total contents in soil for the *Alliaria*
 341 and *Quercus* genera are compared in Fig. 8. These 2 genera were compared because they had the lowest
 342 (*Alliaria*) and the highest (*Quercus*) correlation values of all the genera studied (presented in Fig. S2).
 343 Concerning *Alliaria*, few anticorrelations were found between Cd, Pb, Sn and Zn soil contents and Mn
 344 leaf contents and between As soil contents and P leaf contents. Correlation coefficients were low, with
 345 r values of -0.28 to -0.38 for Mn and -0.26 for P. For other nutrients, there were no highlighted links,
 346 but there were positive correlations with Mg (r = 0.27 to 0.29 for Ni, Pb, Sn and Zn soil contents), S (r
 347 = 0.31 to 0.35 for Cd, Pb, Sn and Zn soil contents) and Zn (r = 0.31 to 0.41 for Cd, Ni, Pb, Sn and Zn
 348 soil contents). Soil TE contents were more strongly related to nutrient contents for the *Quercus* genus
 349 than for *Alliaria*. Indeed, Cu, Fe, K, Mg, Mn, P, S and Zn plant contents were negatively correlated with
 350 As, Cd, Ni and Zn soil contents (and with Sn for K, Mn and P). The correlation coefficients were higher
 351 for *Quercus* than *Alliaria*, with r values that varied from -0.43 to -0.69 for Fe, K, Mg, P and Zn and from
 352 -0.69 to -0.86 for Cu and S.



353
 354 Fig. 8. Correlation matrix of nutrient leaf contents and total TE contents for the *Alliaria* (A) and *Quercus* (B) genera. The
 355 Spearman correlation coefficient is shown only for tests with a p value < 0.05. L: Leaf contents; T: Total contents in soil.

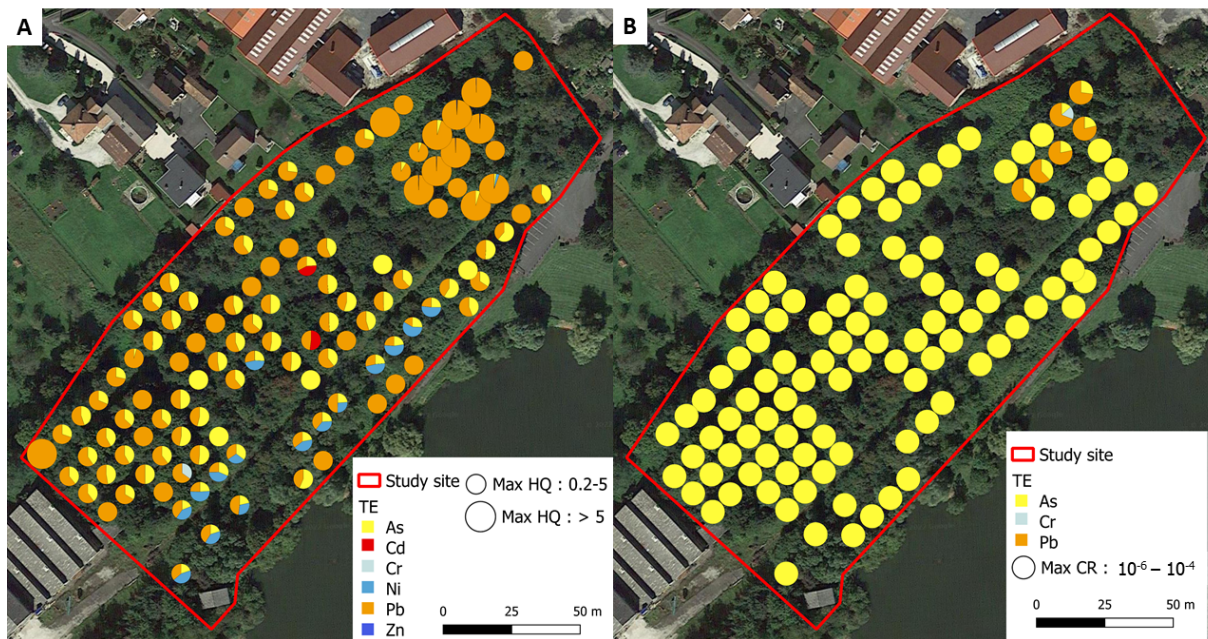
356 For other nutrients, the data did not show noteworthy links with soil contents, with only 2 positive
 357 correlations between Na leaf contents and As and Zn soil contents (r = 0.63 and 0.68, respectively). In

358 general, the anticorrelations with nutrients were higher for As, Ni and Zn than for Cd and higher for Cd
359 than for Sn.

360 Based on the TE contents in the plants and soil TE contents, the HQ and CR were calculated, and their
361 values were mapped (Fig. 9). For the soil and leaf ingestion scenarios, most of the sampling areas had a
362 maximal HQ between 0.2 and 5 across the site (117/125 areas) and were considered to have a possible
363 risk for human health. Pb and As were the elements with the highest number of areas with possible risk
364 (101 and 87 areas, respectively), followed by Ni (19 areas), with the areas of risk mainly distributed
365 close to the pond; other elements had lower numbers of areas with possible risk with 6 areas for Zn, 5
366 areas for Cd and 2 areas for Cr (Fig. 9A). In comparison, only 8 areas had values < 0.2 for all elements
367 and were therefore considered to have no risk (data not shown). In addition, 11 sampling areas had
368 maximal HQ values between 5 and 170 and were therefore considered to have an identified risk (Table
369 S3). One of these areas with high HQ values was localized close to the factory (west), while the others
370 were all in the most contaminated part of the site (north-east). Pb was the only element with $HQ > 5$ and
371 therefore justifies the risk in these areas. However, in the most contaminated area, a possible risk was
372 also detected for As in 7 areas with HQ values between 0.2 and 5, as well as for Zn (6 areas), Cd (3
373 areas), Ni (3 areas) and Cr (1 area).

374 Concerning CR, there was no risk identified in 14 areas (values $< 10^{-6}$). All the other areas (111 areas)
375 had a possible risk due to values ranging from 10^{-6} to 10^{-4} (Fig. 9B). The elevated CR values were often
376 due to As throughout the site, with a maximal value that reached 3.91×10^{-5} , except in the most
377 contaminated area, where Pb (6 areas) and Cr (1 area) also had high CR values that reached 6.21×10^{-5}
378 and 1.51×10^{-5} , respectively.

379 A comparison of the two scenarios showed that soil ingestion contributed more than plant consumption
380 to the HQ and CR values (Table S2). Indeed, for the plant consumption scenario, only 4 HQ values
381 exceeded 0.2 for Cd and Cr (max = 0,61 for Cd), and only 1 CR value exceeded 10^{-6} for Cr (CR =
382 1.32×10^{-5}). Concerning the soil ingestion scenario, HQ values exceeded 0.2 in 109 areas for Pb (11 areas
383 with $HQ > 5$), followed by As (86 areas), Ni (18 areas), Zn (6 areas) and Cd (3 areas), and Cr values
384 exceeded 10^{-6} in 110 areas for As and 6 areas for Pb.



385

386 *Fig. 9. Location and ranges of HQ (A) and CR (B) values calculated at the study site. For each sampling area, a pie chart*
 387 *compared the HQ or CR values associated with each element. The size of the pie chart represents the HQ or CR value of the*
 388 *element with the highest risk. The values below 0.2 for the HQ and 10^{-6} for the CR are not shown on the map.*

389

390 4 Discussion

391 4.1 TE contamination and its impact on floristic diversity and plants

392 Among the main contaminants described in Fig. 2, all had maximal content values at the site that far
393 exceeded the average TE values in surface soil described by [Kabata-Pendias \(2011\)](#). Indeed, the average
394 values commonly reported were 70, 0.41, 27, 2.5, 0.07, 29 and 6.83 mg.kg⁻¹ for Zn, Cd, Pb, Sn, Hg, Ni
395 and As, respectively. Therefore, this contamination had an effect on the floristic composition of the
396 study site. Indeed, the herbaceous families Asteraceae, Poaceae and Fabaceae and tree family
397 Salicaceae, which were the dominant plant families at the study site, have also been reported as the main
398 families at a naturally recolonized industrial site contaminated with Mn, Fe, Cu and Zn in France
399 ([Zapata-Carbonell et al., 2019](#)). More specifically, 23 species were shared by the two industrial
400 wastelands. These families have also been described as dominant in several other sites contaminated by
401 various TEs, such as As, Pb and Cd in Mexico ([Salas-Luévano et al., 2017](#)) and Zn, Cu, Ni and Cr in
402 Cameroon ([Anne et al., 2021](#)), although with fewer shared species (2 and 1, respectively). Our results
403 confirm that TE tolerance, regardless of the element considered, is common in species belonging to
404 these families.

405 However, the composition of the plant communities found on the wasteland differed between the
406 different areas studied. Indeed, two factors structured these communities. The first factor is the type of
407 area, the plant communities are not the same between open and undergrowth areas. This is a logical
408 conclusion since the plants composing the ecosystems have ecological requirements for development,
409 such as light intensity, temperature or humidity ([Syed et al., 2018](#)). The second factor is the level of
410 contamination, highlighted in zones 1 and 5, which were the most contaminated UZ and OZ,
411 respectively. The disappearance of species sensitive to TEs along a contamination gradient on a
412 wasteland has already been reported by [Dazy et al. \(2009\)](#). However, our data also showed a decrease
413 in the vegetation cover of some families, even the most represented ones such as Asteraceae, Fabaceae
414 and Rosaceae. In contrast, coverage for some families, especially Araliaceae, Rubiaceae and Urticaceae,
415 increased with increasing levels of contamination. This is explained by the replacement of species that
416 do not tolerate high levels of TEs by new species and by an increase in the abundance of other species,

417 such as *U. dioica* and *H. helix*, that are more tolerant. Therefore, the contamination level led to a
418 selection of communities based on tolerance to contaminants. As hypothesized, the level of
419 contaminants at the site was a factor that modified the composition of plant communities.

420 As a consequence, the TE contents in soils explained most of the variation observed for the four
421 biodiversity indices. Indeed, while the lower biodiversity in the UZ than in the OZ was related to the
422 area type, the environmental impacts of contaminants were highlighted by the lower biodiversity indices
423 found in the most contaminated UZ (except zone 3) and OZ areas. These decreases were related to the
424 modifications of the plant communities resulting in the presence of fewer but more abundant species.
425 Indeed, TEs are well known to inhibit plant growth and alter plant communities by selecting tolerant
426 species (Muszynska & Labudda, 2019), thus inducing a reduction in plant biodiversity (Alsherif et al.,
427 2022). More specifically, our data showed that Zn and Ni had the greatest impact on biodiversity for
428 both the UZ and OZ based on the anticorrelations with extractable contents. Cd, Sn and Pb also showed
429 anticorrelation but only for OZ. Zone 3 showed a high percentage of bare soil and therefore low
430 biodiversity indices (with high variability), while contaminant levels were comparable with that in zones
431 2 and 4. This could be explained by the heterogeneous pH values in this part of the site, varying from
432 3.95 (minimal pH value on site) to 7, with pH being one of the major soil parameters influencing metal-
433 tolerant plant communities, as shown by Conesa et al. (2007).

434 In addition to influencing biodiversity, TE contents also modified nutrient uptake, as shown by
435 anticorrelations between TE contents in soil and Cu, Fe, K, Mg, Mn, P, S, Zn contents in the leaves of
436 *Quercus* species (Fig. 8). These differences can be explained by the mechanisms involved in the uptake
437 of nonessential TEs by plants. Indeed, these elements can enter the plant through nonspecific pathways
438 by substituting other divalent cations, such as Ca^{2+} , Cu^{2+} , Mg^{2+} , Fe^{2+} and Zn^{2+} (Rascio & Navari-Izzo,
439 2011; Tibbett et al., 2021), and the effect depends on the element and the plant considered (Boechat et
440 al., 2016). Indeed, for the most accumulative species found at the site, *A. petiolata*, few effects were
441 shown and only for Mn uptake. The tolerance and accumulation capacities are usually explained by the
442 overexpression of genes encoding transmembrane transporters, proteins involved in the responses to
443 oxidative stress and synthesis of metal chelators in accumulator species (Rascio & Navari-Izzo, 2011;

444 [Corso & Garcia de la Torre, 2020](#)). The genomic study of *A. petiolata* would allow us to better
445 understand the mechanisms involved in these metal-accumulating species, which should receive
446 attention.

447 4.2 TE accumulation in plants with a special emphasis on *Alliaria petiolata*

448 Overall, Zn, Cd and Ni were the most accumulated elements in plant leaves at the site because the CaCl₂
449 extractable fraction of these elements was higher than that for the other elements, e.g., Pb and Sn. The
450 anticorrelations between the availability percentage and the pH value in soil for Zn, Cd and Ni supported
451 this assumption. Indeed, the soil pH value has a strong influence on the availability of these
452 contaminants, and a decrease in the pH value induces an increase in the extractable CaCl₂ content, as
453 previously described by other authors ([Kashem & Singh, 2001](#); [Spurgeon et al., 2006](#); [Gandois et al.,](#)
454 [2010](#)). Therefore, the pH indirectly affected Zn, Cd and Ni plant contents by solubilizing them in soil.

455 Therefore, of the major contaminants studied at the site, Zn, Cd and Ni were the most heavily
456 accumulated in plants. In particular, the following genera tended to accumulate one or more of these
457 contaminants: *Alliaria* (Zn, Cd, Ni), *Betula* (Zn), *Populus* (Zn, Cd), *Salix* (Zn, Cd) and *Urtica* (Zn). The
458 *Betula*, *Populus* and *Salix* genera are known to contain species with accumulation capacities for Zn
459 and/or Cd ([Margui et al., 2007](#); [Migeon et al., 2009](#); [Bissonnette et al., 2010](#); [Mrnka et al., 2012](#);
460 [Dmuchowski et al. 2014](#)), including several species found at the study site (*P. nigra*, *P. tremula*, *S. alba*,
461 *S. fragilis*, *S. purpurea*, *S. viminalis*) ([Marmioli et al., 2011](#)). [Migeon et al. \(2009\)](#) found Zn contents
462 varying from 200 to 950 mg.kg⁻¹ DW in the genera *Betula*, *Salix* and *Populus* at a Zn-, Pb- and Cd-
463 contaminated site, which is similar to our data. However, much higher contents can be found in the
464 literature, as for the species *Salix aquatica grandis*, which can reach 2800 mg.kg⁻¹ DW for Zn and 128
465 mg.kg⁻¹ DW for Cd ([Ciadamidaro et al. 2019](#)). These genera are therefore frequently studied in
466 phytoremediation because of their interesting capacities ([Mleczek et al., 2010](#); [Lewis et al., 2015](#); [Dadea](#)
467 [et al., 2017](#); [Kubatova et al., 2022](#); [Yi et al., 2022](#); [Yin et al., 2022](#)). In contrast, the other genera
468 contained low leaf contents, especially *Ailanthus*, *Fraxinus* and *Prunus*, as found previously ([Migeon et](#)
469 [al., 2009](#)).

470 Fe, Cu and Mn were also found to be transferred to the leaves, which seems rational since these are
471 essential elements for plants (Fernando et al., 2016; Lange et al., 2017; Naranjo-Arcos et al., 2017).
472 However, Mn values exceeded the normal leaf content range of 30-300 mg.kg⁻¹ DW described by
473 Kabata-Pendias (2011), especially in samples from the genera *Acer* and *Quercus*. Comparable Mn
474 concentrations have been reported by Stanković et al. (2011), with mean values that ranged between 370
475 and 550 and 67 and 285 mg.kg⁻¹ DW for *Quercus petraea* and *Acer campestre* species, respectively,
476 species that are also present at our study site. Fernando et al. (2016) found Mn contents that reached
477 2600 mg.kg⁻¹ DW for *Acer rubrum* (similar to our data) and even higher maximal contents in *Acer*
478 *saccharum*, with a value of 4300 mg.kg⁻¹ DW. Concerning the *Quercus* genus, Huang et al. (2014) found
479 contents of 800 mg.kg⁻¹ DW, with a maximal value of 2700 mg.kg⁻¹ DW in *Quercus alba* on an Mn
480 mining site, which was almost twice as high as the values found for *Quercus* species at our study site.
481 All of these data highlight that accumulation capacities of Mn, Zn and Cd can vary greatly from one
482 species to another, even within the same genus.

483 Hg, Sn and Cr were not found in the leaves of any of the tree, shrub or herbaceous species studied. These
484 results are consistent with the contents of these elements found in the soil CaCl₂ extractable fraction,
485 which were less than the LQ for most of the samples. Several studies on the chemical distributions of
486 Pb and As have highlighted that the exchangeable fraction of these elements was lower than that of other
487 TEs, such as Cd or Zn (Pichtel et al., 2000; Qasim et motelica-Heino, 2014; Gankhurel et al., 2020).
488 Indeed, depending on the soil, Pb and As could be bound to carbonate, Fe-Mn oxides, organic matter
489 and/or in residual fractions that are harder to extract and therefore less mobile (Angelova et al., 2004;
490 Qasim & Motelica-Heino, 2014) and hence poorly transferred to plant tissues.

491 The dominant species of the site, *A. petiolata*, which belongs to the Brassicaceae family, showed the
492 highest levels of TEs in its leaves. The Brassicaceae family is known to contain 25% of the metal-
493 hyperaccumulating species described (Gall & Rajakaruna, 2013; Suman et al., 2018), which are more
494 tolerant to metal contamination. *A. petiolata* does not seem to differ from this general feature. To our
495 knowledge, few studies have been conducted on TE contents in this species, with lower values reported
496 than in our study for Zn. Grabner et al. (2011) found maximal contents of 393 mg.kg⁻¹ DW for Zn and

497 2.1 mg.kg⁻¹ for Cd at contaminated sites. Furthermore, the translocation ratio (ratio between shoot and
498 root contents) was higher than 1 for Zn, Cd and Ni (Grabner et al., 2011; Drozdova et al., 2019),
499 indicating that this species has the capacity to concentrate these three contaminants in its aerial parts.
500 Moreover, the use of *A. petiolata* in phytoextraction strategies has been suggested by Drozdova et al.
501 (2019), and the maximal Zn and Ni values found in the present study were much higher than the
502 previously published data, supporting this potential. In addition, this plant is fast growing and produces
503 a high biomass, which has interesting implications for phytoextraction (Grabner et al., 2011).

504 *A. petiolata* was also demonstrated to be a relevant Zn bioindicator, being distributed throughout the
505 site. Indeed, Zn accumulation in the leaves of this species was correlated with the CaCl₂ extractable
506 fractions. These features are usually described to consider a plant as a metal bioindicator (Kabata-
507 Pendias, 2011).

508 4.3 Impact of TEs on human health

509 The HQ and CR calculated for several parts of the site showed that the TE contents could have an impact
510 on human health depending on the soil and plant ingestion scenarios considered. For most of the areas,
511 a possible risk was identified due to Pb and As based on the HQ and CR values. These two elements are
512 known to be particularly toxic to humans either by disturbing metabolism or being carcinogenic (Turdi
513 & Yang, 2016). The element that presented the highest risk at the site for both HQ and CR is Pb,
514 especially in the soil ingestion scenario, due to its high total contents in soil relative to its toxicity.
515 Indeed, even if this element was the second most abundant after Zn, it would remain the greatest threat
516 since its toxicity is a thousand times higher than that of Zn. However, in our study site, the low
517 bioavailability of Pb prevented it from accumulating in plants to levels that are dangerous for humans
518 in the scenarios considered; nevertheless, the maximal contents found reached the tolerable limit for the
519 crops described by Kabata-Pendias (2011), which varies from 0.5 to 10. The low contents available for
520 plants have often been reported in the literature for this element, as previously explained in section 4.2.
521 Although Pb is the element with the highest risk values at the site, As is the element that most frequently
522 exceeded the boundary between no risk and possible risk. Although this element had no HQ or CR

523 values high enough to identify it as a risk, there is a possible risk in almost all the areas studied. This is
524 explained by the high levels of As throughout the site, with more than 60% of the areas studied having
525 total As contents in soil that exceed 40 mg.kg⁻¹ DW. Indeed, these values are almost 6 times higher than
526 the world soil average of 6.8 mg.kg⁻¹ identified by [Kabata-Pendias \(2011\)](#).

527 On the other hand, for Cd and Cr, although most of the areas had HQ and CR values < 0.2, the contents
528 in leaves of *A. petiolata* presented a potential risk for humans in the case of consumption for 4 areas at
529 the site. Human exposure to these elements via consumption of metal-accumulating plants in
530 contaminated sites has already been described as potentially toxic ([Naz et al., 2020](#)). Concerning Cr, the
531 risk values exceeded 0.2 for only a few parts of the site because most plant sample contents were below
532 the LQ. Nevertheless, even low contents (18 to 25 mg.kg⁻¹ DW) were sufficient to consider a possible
533 risk, indicating that this TE should be taken into consideration even at low levels in plants as should its
534 bioavailability. Cd is considered one of the elements with the most toxic effects on human, animal and
535 plant biological processes ([Diatta et al., 2003](#); [Kabata-Pendias, 2011](#)). [Antoine et al. \(2017\)](#) reported that
536 Cd was responsible for higher HQ than As, Al, and Pb in several food crops tested. Our data also showed
537 that this element had the highest risk in the plant exposure scenario. This can be explained by the
538 efficient mechanisms for the uptake and translocation of Cd in plants, although it is not essential, which
539 leads to high concentrations in aerial plant parts ([Naz et al., 2020](#)). Consequently, although few areas of
540 the site showed a possible risk for Cd, its bioavailability needs to be monitored, especially under high
541 pH variation, as in our study site. Indeed, pH can greatly increase the Cd contents accumulated in aerial
542 plant parts and thus the risk from consumption.

543 Overall, the modification of nutrient contents in plants and the measurement of HQ and CR showed that
544 TE contamination had an effect on the environment at the study site. These results highlight the human
545 and environmental risks and the necessity to manage the study site and similar marginal lands to restore
546 interest and uses to these sites.

547

548 **5 Conclusions**

549 The soils of the industrial wasteland located in Vieux-Charmont presented contamination with several
550 TEs, with heterogeneous TE contents and pH values. This has led to the presence of environments with
551 similar abiotic conditions but with modified floristic compositions. Moreover, this study highlighted
552 differences in the accumulation of TEs with the vegetation of the site, depending on the genus
553 considered. One of these species, *A. petiolata*, is also a potential bioindicator of Zn that could provide
554 information about the mobility and spreading risk of this element in ecosystems, especially since the
555 species grows easily in contaminated environments. The accumulation capacities of this species, as well
556 as others on the site, notably those belonging to *Salix*, *Populus* and *Betula*, allow us to consider the
557 possibility of using these indigenous species for managing the site by phytoremediation techniques such
558 as phytoextraction to reduce the quantity of contaminants in the soil. These techniques are low-cost and
559 non-invasive ways to use plants to manage site contamination (Peer et al., 2005). Moreover, it may be
560 possible to use marginal lands for economic purposes and to restore some ecosystem services. The level
561 of contamination in the soil and vegetation as well as the measurement of the associated HQ and CR
562 also make it possible to decide and locate the necessary actions for the future of the site. Indeed, the
563 measurement of human health risks is fundamental because the long-term objective is to open a part of
564 the site as an educational park with communication about the research conducted for the public.

565 **Funding**

566 The project ECOPOLIS has received funding from the Agence Nationale de la Recherche (ANR) under
567 ANR-20-CE22-0010 and from the French General Secretariat for Investment, under grant “Territory of
568 Innovation” of the Investment for the Future Program (PIA3) and by the Pays de Montbéliard
569 Agglomération under the Ph-D grant for JC. We thank Pays de Montbéliard Agglomération for allowing
570 access to the Vieux-Charmont site.

571 **Acknowledgments**

572 We acknowledge Dr. Nadia Morin-Crini, and Caroline Amiot of the PEAT² platform for ICP analyses.

573 **References**

- 574 Ali, H., Khan, E., Sajad, M.A., 2013. Phytoremediation of heavy metals—Concepts and applications.
575 Chemosphere 91, 869–881. <https://doi.org/10.1016/j.chemosphere.2013.01.075>
- 576 Alloway, B.J., 2013. Chapter 7 Heavy Metals and Metalloids as Micronutrients for Plants and Animals,
577 in: Alloway, B.J. (Ed.), Heavy Metals in Soils, Environmental Pollution. Springer Netherlands,
578 Dordrecht, pp. 195–209. https://doi.org/10.1007/978-94-007-4470-7_7
- 579 Alsherif, E.A., Al-Shaikh, T.M., AbdElgawad, H., 2022. Heavy Metal Effects on Biodiversity and Stress
580 Responses of Plants Inhabiting Contaminated Soil in Khulais, Saudi Arabia. Biology 11, 21.
581 <https://doi.org/10.3390/biology11020164>
- 582 Angelova, V., Ivanov, K., Ivanova, R., 2004. Effect of Chemical Forms of Lead, Cadmium, and Zinc in
583 Polluted Soils on Their Uptake by Tobacco. Journal of Plant Nutrition 27, 757–773.
584 <https://doi.org/10.1081/PLN-120030609>
- 585 Anne, A., Ebenezer, S.K., Guy Valerie, D.W., Pierre, N., Cédric, D.C., Annie Stephanie, N., Pierre
586 François, D., Noumsi Ives Magloire (In memorium), K., 2021. Floristic surveys of some lowlands
587 polluted of a tropical urban area: the case of Yaounde, Cameroon. International Journal of
588 Phytoremediation 23, 1191–1202. <https://doi.org/10.1080/15226514.2021.1884183>
- 589 Antoine, J.M.R., Fung, L.A.H., Grant, C.N., 2017. Assessment of the potential health risks associated
590 with the aluminium, arsenic, cadmium and lead content in selected fruits and vegetables grown in
591 Jamaica. Toxicology Reports 4, 181–187. <https://doi.org/10.1016/j.toxrep.2017.03.006>
- 592 Arora, M., Kiran, B., Rani, S., Rani, A., Kaur, B., Mittal, N., 2008. Heavy metal accumulation in
593 vegetables irrigated with water from different sources. Food Chemistry 111, 811–815.
594 <https://doi.org/10.1016/j.foodchem.2008.04.049>
- 595 Assad, M., Tatin-Froux, F., Blaudez, D., Chalot, M., Parelle, J., 2017. Accumulation of trace elements
596 in edible crops and poplar grown on a titanium ore landfill. Environmental Science Pollution Research
597 24, 5019–5031. <https://doi.org/10.1007/s11356-016-8242-4>

598 Aycicek, M., Kaplan, O., Yaman, M., 2008. Effect of Cadmium on Germination, Seedling Growth and
599 Metal Contents of Sunflower (*Helianthus annuus* L.). *Asian Journal of Chemistry* 20, 11.

600 Barbillon, A., Aubry, C., Manouchehri, N., 2019. Guide R.E.F.U.G.E. Caractérisation de la
601 contamination des sols urbains destinés à la culture maraîchère et évaluation des risques sanitaires. Cas
602 de la région Île-de-France. https://www.inrae.fr/sites/default/files/guide_refuge.pdf

603 Bissonnette, L., St-Arnaud, M., Labrecque, M., 2010. Phytoextraction of heavy metals by two
604 Salicaceae clones in symbiosis with arbuscular mycorrhizal fungi during the second year of a field trial.
605 *Plant Soil* 332, 55–67. <https://doi.org/10.1007/s11104-009-0273-x>

606 Boechat, C.L., Carlos, F.S., Gianello, C., de Oliveira Camargo, F.A., 2016. Heavy Metals and Nutrients
607 Uptake by Medicinal Plants Cultivated on Multi-metal Contaminated Soil Samples from an Abandoned
608 Gold Ore Processing Site. *Water, Air & Soil Pollution* 227, 11. <https://doi.org/10.1007/s11270-016-3096-4>

609 Ciadamidaro, L., Parelle, J., Tatin-Froux, F., Moyen, C., Durand, A., Zappelini, C., Morin-Crini, N.,
610 Soupe, D., Blaudez, D., Chalot, M., 2019. Early screening of new accumulating versus non-
611 accumulating tree species for the phytomanagement of marginal lands. *Ecological Engineering* 130,
612 147–156. <https://doi.org/10.1016/j.ecoleng.2019.02.010>

613 Conesa, H.M., García, G., Faz, Á., Arnaldos, R., 2007. Dynamics of metal tolerant plant communities'
614 development in mine tailings from the Cartagena-La Unión Mining District (SE Spain) and their interest
615 for further revegetation purposes. *Chemosphere* 68, 1180–1185.
616 <https://doi.org/10.1016/j.chemosphere.2007.01.072>

617 Corso, M., García de la Torre, V.S., 2020. Biomolecular approaches to understanding metal tolerance
618 and hyperaccumulation in plants. *Metallomics* 12, 840–859. <https://doi.org/10.1039/d0mt00043d>

619 Dadea, C., Russo, A., Tagliavini, M., Mimmo, T., Zerbe, S., 2017. Tree Species as Tools for
620 Biomonitoring and Phytoremediation in Urban Environments: A Review with Special Regard to Heavy
621 Metals. *Arboriculture & Urban Forestry* 43, 155–167. <https://doi.org/10.48044/jauf.2017.014>

622 Dazy, M., Béraud, E., Cotelte, S., Grévilliot, F., Férard, J.-F., Masfaraud, J.-F., 2009. Changes in plant
623 communities along soil pollution gradients: Responses of leaf antioxidant enzyme activities and
624 phytochelatin contents. *Chemosphere* 77, 376–383. <https://doi.org/10.1016/j.chemosphere.2009.07.021>

625 De Mendiburu F., 2021. agricolae: Statistical Procedures for Agricultural Research. R package version
626 1.3-5. <https://CRAN.R-project.org/package=agricolae>

627 Dehghani, S., Moore, F., Vasiluk, L., Hale, B.A., 2018. The influence of physicochemical parameters
628 on bioaccessibility-adjusted hazard quotients for copper, lead and zinc in different grain size fractions
629 of urban street dusts and soils. *Environmental Geochemistry and Health* 40, 1155–1174.
630 <https://doi.org/10.1007/s10653-017-9994-6>

631 Diatta, J.B., Grzebisz, W., Apolinarska, K., 2003. A study of soil pollution by heavy metals in the city
632 of Poznan (Poland) using dandelion (*Taraxacum officinale* Web) as a bioindicator. *Electronic Journal*
633 *of Polish Agricultural Universities* 6, 9.

634 Dmuchowski, W., Gozdowski, D., Brągoszewska, P., Baczewska, A.H., Suwara, I., 2014.
635 Phytoremediation of zinc contaminated soils using silver birch (*Betula pendula* Roth). *Ecological*
636 *Engineering* 71, 32–35. <https://doi.org/10.1016/j.ecoleng.2014.07.053>

637 Drozdova, I., Alekseeva-Popova, N., Dorofeyev, V., Bech, J., Belyaeva, A., Roca, N., 2019. A
638 comparative study of the accumulation of trace elements in Brassicaceae plant species with
639 phytoremediation potential. *Applied Geochemistry* 108, 7. <https://doi.org/10.1016/j.apgeochem.2019.104377>

640 Favas, P.J.C., Pratas, J., Prasad, M.N.V., 2012. Accumulation of arsenic by aquatic plants in large-scale
641 field conditions: Opportunities for phytoremediation and bioindication. *Science of The Total*
642 *Environment* 433, 390–397. <https://doi.org/10.1016/j.scitotenv.2012.06.091>

643 Fernando, D.R., Marshall, A.T., Lynch, J.P., 2016. Foliar Nutrient Distribution Patterns in Sympatric
644 Maple Species Reflect Contrasting Sensitivity to Excess Manganese. *PLOS ONE* 11, 17.
645 <https://doi.org/10.1371/journal.pone.0157702>

646 Gall, J.E., Rajakaruna, N., 2013. Chapter 6 The physiology, functional genomics, and applied ecology
647 of heavy metal-tolerant Brassicaceae, in: Brassicaceae Characterization, Functional Genomics and
648 Health Benefits. Minglin Lang, New York, pp. 121–148.

649 Gandois, L., Probst, A., Dumat, C., 2010. Modelling trace metal extractability and solubility in French
650 forest soils by using soil properties. *European Journal of Soil Science* 61, 271–286.
651 <https://doi.org/10.1111/j.1365-2389.2009.01215.x>

652 Gankhurel, B., Fukushi, K., Akehi, A., Takahashi, Y., Zhao, X., Kawasaki, K., 2020. Comparison of
653 Chemical Speciation of Lead, Arsenic, and Cadmium in Contaminated Soils from a Historical Mining
654 Site: Implications for Different Mobilities of Heavy Metals. *ACS Earth and Space Chemistry* 4, 1064–
655 1077. <https://doi.org/10.1021/acsearthspacechem.0c00087>

656 Grabner, B., Ribarič-Lasnik, C., Romih, N., Pfeifhofer, H.W., Batič, F., 2011. Bioaccumulation
657 Capacity for Pb, Cd and Zn from Polluted Soil in Selected Species of the Brassicaceae Family Growing
658 in Different Vegetation Types. *Phyton; Annales Rei Botanicae* 50, 287–300.

659 Harrell F.E., 2022. Hmisc: Harrell Miscellaneous. R package version 4.7-1. [https://CRAN.R-](https://CRAN.R-project.org/package=Hmisc)
660 [project.org/package=Hmisc](https://CRAN.R-project.org/package=Hmisc)

661 Houba, V.J.G., Lexmond, Th.M., Novozamsky, I., van der Lee, J.J., 1996. State of the art and future
662 developments in soil analysis for bioavailability assessment. *Science of The Total Environment* 178,
663 21–28. [https://doi.org/10.1016/0048-9697\(95\)04793-X](https://doi.org/10.1016/0048-9697(95)04793-X)

664 Huang, J., Nara, K., Zong, K., Wang, J., Xue, S., Peng, K., Shen, Z., Lian, C., 2014. Ectomycorrhizal
665 fungal communities associated with Masson pine (*Pinus Massoniana*) and white oak (*Quercus fabri*) in
666 a manganese mining region in Hunan Province, China. *Fungal ecology* 9, 10.
667 <https://doi.org/10.1016/j.funeco.2014.01.001>

668 Jabeen, R., Ahmad, A., Iqbal, M., 2009. Phytoremediation of Heavy Metals: Physiological and
669 Molecular Mechanisms. *The Botanical Review* 75, 339–364. <https://doi.org/10.1007/s12229-009-9036-x>

670 Jónsson, J.Ö.G., Davíðsdóttir, B., 2016. Classification and valuation of soil ecosystem services.
671 *Agricultural Systems* 145, 24–38. <https://doi.org/10.1016/j.agsy.2016.02.010>

672 Kabata-Pendias, A., 2011. Trace elements in soils and plants, 4th edition ed. CRC Press, Boca Raton.

673 Kashem, M.A., Singh, B.R., 2001. Metal availability in contaminated soils: I. Effects of flooding and
674 organic matter on changes in Eh, pH and solubility of Cd, Ni and Zn. *Nutrient Cycling in*
675 *Agroecosystems* 61, 247–255. <https://doi.org/10.1023/A:1013762204510>

676 Kubátová, P., Žilincíková, N., Száková, J., Zemanová, V., Tlustoš, P., 2022. Is the harvest of *Salix* and
677 *Populus* clones in the growing season truly advantageous for the phytoextraction of metals from a long-
678 term perspective? *Science of The Total Environment* 838, 9. <https://doi.org/10.1016/j.scitotenv.2022.156630>

679 Lange, B., Van der Ent, A., Baker, A.J.M., Echevarria, G., Mahy, G., Malaisse, F., Meerts, P., Pourret,
680 O., Verbruggen, N., Faucon, M.-P., 2017. Copper and cobalt accumulation in plants: a critical
681 assessment of the current state of knowledge. *New phytologist* 213, 537–551.
682 <https://doi.org/10.1111/nph.14175>

683 Lewis, J., Qvarfort, U., Sjöström, J., 2015. *Betula pendula*: A Promising Candidate for Phytoremediation
684 of TCE in Northern Climates. *International Journal of Phytoremediation* 17, 9–15.
685 <https://doi.org/10.1080/15226514.2013.828012>

686 Marguá, E., Queralt, I., Carvalho, M.L., Hidalgo, M., 2007. Assessment of metal availability to
687 vegetation (*Betula pendula*) in Pb-Zn ore concentrate residues with different features. *Environmental*
688 *Pollution* 145, 179–184. <https://doi.org/10.1016/j.envpol.2006.03.028>

689 Marmiroli, M., Pietrini, F., Maestri, E., Zacchini, M., Marmiroli, N., Massacci, A., 2011. Growth,
690 physiological and molecular traits in Salicaceae trees investigated for phytoremediation of heavy metals
691 and organics. *Tree Physiology* 31, 1319–1334. <https://doi.org/10.1093/treephys/tpr090>

692 MEEM, 2017. *Méthodologie nationale de gestion des sites et sols pollués*. Direction générale de la
693 prévention des risques. Ministère de l'environnement, de l'énergie et de la mer, Paris, 128. [https://ssp-](https://ssp-infoterre-refonte.brgm.fr/fr/methodologie/methodologie-nationale-gestion-ssp)
694 [infoterre-refonte.brgm.fr/fr/methodologie/methodologie-nationale-gestion-ssp](https://ssp-infoterre-refonte.brgm.fr/fr/methodologie/methodologie-nationale-gestion-ssp)

695 Migeon, A., Richaud, P., Guinet, F., Chalot, M., Blaudez, D., 2009. Metal Accumulation by Woody
696 Species on Contaminated Sites in the North of France. *Water, Air, and Soil Pollution* 204, 89–101.
697 <https://doi.org/10.1007/s11270-009-0029-5>

698 Mleczek, M., Rutkowski, P., Rissmann, I., Kaczmarek, Z., Golinski, P., Szentner, K., Strażyńska, K.,
699 Stachowiak, A., 2010. Biomass productivity and phytoremediation potential of *Salix alba* and *Salix*
700 *viminalis*. *Biomass and Bioenergy* 34, 1410–1418. <https://doi.org/10.1016/j.biombioe.2010.04.012>

701 Morel, J.L., Chenu, C., Lorenz, K., 2015. Ecosystem services provided by soils of urban, industrial,
702 traffic, mining, and military areas (SUITMAs). *Journal of Soils and Sediments* 15, 1659–1666.
703 <https://doi.org/10.1007/s11368-014-0926-0>

704 Mrnka, L., Kuchár, M., Cieslarová, Z., Matějka, P., Száková, J., Tlustoš, P., Vosátka, M., 2012. Effects
705 of Endo- and Ectomycorrhizal Fungi on Physiological Parameters and Heavy Metals Accumulation of
706 Two Species from the Family Salicaceae. *Water, Air, & Soil Pollution* 223, 399–410.
707 <https://doi.org/10.1007/s11270-011-0868-8>

708 Muszyńska, E., Labudda, M., 2019. Dual Role of Metallic Trace Elements in Stress Biology—From
709 Negative to Beneficial Impact on Plants. *International Journal of Molecular Sciences* 20, 27.
710 <https://doi.org/10.3390/ijms20133117>

711 Naranjo-Arcos, M.A., Maurer, F., Meiser, J., Pateyron, S., Fink-Straube, C., Bauer, P., 2017. Dissection
712 of iron signaling and iron accumulation by overexpression of subgroup Ib bHLH039 protein. *Scientific*
713 *Reports* 7, 12. <https://doi.org/10.1038/s41598-017-11171-7>

714 Naz, A., Chowdhury, A., Chandra, R., Mishra, B.K., 2020. Potential human health hazard due to
715 bioavailable heavy metal exposure via consumption of plants with ethnobotanical usage at the largest
716 chromite mine of India. *Environmental Geochemistry and Health* 42, 4213–4231.
717 <https://doi.org/10.1007/s10653-020-00603-5>

718 Oksanen J., Simpson G.L., Blanchet F.G., Kindt R., Legendre P., Minchin P.R., O'Hara R.B., Solymos
719 P., Stevens M.H.H., Szoecs R., Wagner H., Barbour M., Bedward M., Bolker B., Borcard D., Carvalho
720 G., Chirico M., De Caceres M., Durand S., Evangelista H.B.A., FitzJohn R., Friendly M., Furneaux B.,
721 Hannigan G., Hill M.O., Lahti L., McGlenn D., Ouellette M.H., Cunha E.T., Smith T., Stier A., Ter
722 Braak C.J.F., Weedon J., 2022. vegan: Community Ecology Package. R package version 2.6-2.
723 <https://CRAN.R-project.org/package=vegan>

724 Panagos, P., Van Liedekerke, M., Yigini, Y., Montanarella, L., 2013. Contaminated Sites in Europe:
725 Review of the Current Situation Based on Data Collected through a European Network. *Journal of*
726 *Environmental and Public Health* 2013, 11. <https://doi.org/10.1155/2013/158764>

727 Paya Perez, A., Rodriguez Eugenio, N., 2018. Status of local soil contamination in Europe: Revision of
728 the indicator “Progress in the management contaminated sites in Europe.” Publications Office of the
729 European Union, 193. <https://doi.org/10.2760/093804>

730 Peer, W.A., Baxter, I.R., Richards, E.L., Freeman, J.L., Murphy, A.S., 2005. Phytoremediation and
731 hyperaccumulator plants, in: *Molecular Biology of Metal Homeostasis and Detoxification, Topics in*
732 *Current Genetics*. Springer Berlin Heidelberg, Berlin, Heidelberg, pp. 299–340.

733 Pichtel, J., Kuroiwa, K., Sawyerr, H.T., 2000. Distribution of Pb, Cd and Ba in soils and plants of two
734 contaminated sites. *Environmental Pollution* 110, 171–178. [https://doi.org/10.1016/s0269-7491\(99\)00272-9](https://doi.org/10.1016/s0269-7491(99)00272-9)

735 Prasad, M.N.V., Strzałka, K., 1999. Chapter 6 Impact of Heavy Metals on Photosynthesis, in: *Heavy*
736 *Metal Stress in Plants*. Springer Berlin Heidelberg, Berlin, Heidelberg, pp. 117–138.
737 https://doi.org/10.1007/978-3-662-07745-0_6

738 Qasim, B., Motelica-Heino, M., 2014. Potentially toxic element fractionation in technosoils using two
739 sequential extraction schemes. *Environmental Science and Pollution Research* 21, 5054–5065.
740 <https://doi.org/10.1007/s11356-013-2457-4>

741 Rajaganapathy, V., Xavier, F., Sreekumar, D., Mandal, P.K., 2011. Heavy Metal Contamination in Soil,
742 Water and Fodder and their Presence in Livestock and Products : A Review. *Journal of Environmental*
743 *Science and Technology* 4, 234–249. <https://doi.org/10.3923/jest.2011.234.249>

744 Rascio, N., Navari-Izzo, F., 2011. Heavy metal hyperaccumulating plants: How and why do they do it?
745 And what makes them so interesting? *Plant Science* 180, 169–181.
746 <https://doi.org/10.1016/j.plantsci.2010.08.016>

747 Salas-Luévano, M.A., Mauricio-Castillo, J.A., González-Rivera, M.L., Vega-Carrillo, H.R., Salas-
748 Muñoz, S., 2017. Accumulation and phytostabilization of As, Pb and Cd in plants growing inside mine

749 tailings reforested in Zacatecas, Mexico. *Environmental Earth Sciences* 76, 12.
750 <https://doi.org/10.1007/s12665-017-7139-y>

751 Spurgeon, D.J., Lofts, S., Hankard, P.K., Toal, M., McLellan, D., Fishwick, S., Svendsen, C., 2006.
752 EFFECT OF pH ON METAL SPECIATION AND RESULTING METAL UPTAKE AND TOXICITY
753 FOR EARTHWORMS. *Environmental Toxicology and Chemistry* 25, 788–796. [https://doi.org/10.1897/05-](https://doi.org/10.1897/05-045R1.1)
754 [045R1.1](https://doi.org/10.1897/05-045R1.1)

755 Stanek, E.J., Calabrese, E.J., Zorn, M., 2001. Soil Ingestion Distributions for Monte Carlo Risk
756 Assessment in Children. *Human and Ecological Risk Assessment* 7, 357–368.
757 <https://doi.org/10.1080/20018091094402>

758 Stanković, D., Krstić, B., Šijačić-Nikolić, M., Knežević, M., 2011. Concentrations of manganese and
759 iron in some woody and herbs plants. *Matica Srpska Proceedings for Natural Sciences* 121, 39–49.
760 <https://doi.org/10.2298/ZMSPN1121039S>

761 Suman, J., Uhlik, O., Viktorova, J., Macek, T., 2018. Phytoextraction of Heavy Metals: A Promising
762 Tool for Clean-Up of Polluted Environment? *Frontiers in Plant Science* 9, 15.
763 <https://doi.org/10.3389/fpls.2018.01476>

764 Syed, R., Kapoor, D., Bhat, A.A., 2018. HEAVY METAL TOXICITY IN PLANTS: A REVIEW. *Plant*
765 *archives* 18, 1229–1238.

766 Tano, B.F., Brou, C.Y., Dossou-Yovo, E.R., Saito, K., Futakuchi, K., Wopereis, Marco.C.S., Husson,
767 O., 2020. Spatial and Temporal Variability of Soil Redox Potential, pH and Electrical Conductivity
768 across a Toposequence in the Savanna of West Africa. *Agronomy* 10, 22.
769 <https://doi.org/10.3390/agronomy10111787>

770 Tibbett, M., Green, I., Rate, A., De Oliveira, V.H., Whitaker, J., 2021. The transfer of trace metals in
771 the soil-plant-arthropod system. *Science of The Total Environment* 779, 29.
772 <https://doi.org/10.1016/j.scitotenv.2021.146260>

773 Turdi, M., Yang, L., 2016. Trace Elements Contamination and Human Health Risk Assessment in
774 Drinking Water from the Agricultural and Pastoral Areas of Bay County, Xinjiang, China. *International*
775 *Journal of Environmental Research and Public Health* 13, 15. <https://doi.org/10.3390/ijerph13100938>

776 Verbruggen, N., Hermans, C., Schat, H., 2009. Molecular mechanisms of metal hyperaccumulation in
777 plants. *New Phytologist* 181, 759–776. <https://doi.org/10.1111/j.1469-8137.2008.02748.x>

778 Vidal-beaudet, L., Rossignol, J.-P., 2018. Urban Soils: Artificialization and Management, in: *Soils as a*
779 *Key Component of the Critical Zone 5*. John Wiley & Sons, Inc., Hoboken, NJ, USA, pp. 189–210.
780 <https://doi.org/10.1002/9781119438298.ch8>

781 Warsi, M.K., Howladar, S.M., Alsharif, M.A., 2023. Regulon: An overview of plant abiotic stress
782 transcriptional regulatory system and role in transgenic plants. *Brazilian Journal of Biology* 83, 14.
783 <https://doi.org/10.1590/1519-6984.245379>

784 Wei T., Simko V., 2021. R package “corrplot”: Visualization of a Correlation Matrix (Version 0.92).
785 <https://CRAN.R-project.org/package=corrplot>

786 Wickham H., 2016. *ggplot2: Elegant Graphics for Data Analysis*. Springer-Verlag New York. ISBN 978-3-319-
787 24277-4, <https://ggplot2.tidyverse.org>.

788 Wikum, D.A., Shanholtzer, G.F., 1978. Application of the Braun-Blanquet cover-abundance scale for
789 vegetation analysis in land development studies. *Environmental Management* 2, 323–329.
790 <https://doi.org/10.1007/BF01866672>

791 Wilke C.O., 2020. cowplot: Streamlined Plot Theme and Plot Annotations for “ggplot2”. R package
792 version 1.1.1. <https://CRAN.R-project.org/package=cowplot>

793 Yi, L., Wu, M., Yu, F., Song, Q., Zhao, Z., Liao, L., Tong, J., 2022. Enhanced cadmium
794 phytoremediation capacity of poplar is associated with increased biomass and Cd accumulation under
795 nitrogen deposition conditions. *Ecotoxicology and Environmental Safety* 246, 11.
796 <https://doi.org/10.1016/j.ecoenv.2022.114154>

797 Yin, Z., Yu, J., Han, X., Wang, H., Yang, Q., Pan, H., Lou, Y., Zhuge, Y., 2022. A novel
798 phytoremediation technology for polluted cadmium soil: *Salix integra* treated with spermidine and
799 activated carbon. *Chemosphere* 306, 10. <https://doi.org/10.1016/j.chemosphere.2022.135582>

800 Zapata-Carbonell, J., Bégeot, C., Carry, N., Choulet, F., Delhantal, P., Gillet, F., Girardclos, O., Mouly,
801 A., Chalot, M., 2019. Spontaneous ecological recovery of vegetation in a red gypsum landfill: *Betula*
802 *pendula* dominates after 10 years of inactivity. *Ecological Engineering* 132, 31–40.
803 <https://doi.org/10.1016/j.ecoleng.2019.03.013>

804 Zhang, Q., Wang, C., 2020. Natural and Human Factors Affect the Distribution of Soil Heavy Metal
805 Pollution: a Review. *Water, Air, & Soil Pollution* 231, 350. <https://doi.org/10.1007/s11270-020-04728-2>

806